Diagnosis and optimization of the oil lubrification system

João Pamplona de Puga Coutinho

Master Dissertation

FEUP Supervisor: Prof. Abel Rouboa

Frezite Supervisor: Eng. Diogo Costa

U.PORTO
FEUP FACULDADE DE ENGENHARIA
UNIVERSIDADE DO PORTO

Master in Mechanical Engineering

February 2023

Abstract

Every industry in the world strives to raise production rates while lowering costs at the same time. One of the most popular machining techniques for producing tools with excellent dimensional accuracy and good surface finishes is Grinding. In order to achieve the desired quality and to safeguard the workpiece and the cutting tool or grinding wheel, cutting fluids are also inevitably used to cool and lubricate the tools in production. This is only practical, though, if all conditions are met for the fluid, in this case oil, to travel to the operating machines in the most efficient manner.

This work was developed with the goal of optimizing the lubrication procedure in grinding machines, allowing to increase production effectiveness while at the same time reducing costs involved in the process, making it more sustainable in terms of both the environment and the economy.

This dissertation was created in a real-world setting connected to a cutting tool manufacturing business that made use of its facilities to enhance these parameters.

In the first chapters, the grinding process and the significance of lubrication in this manufacturing process are described theoretically. Additionally, the ideas related to the entire lubrication process are covered, including the pipe-based oil distribution system, the filtering system, and the cooling system. The equipment and devices used in the project are described in the following chapters. After that a diagnosis of the facilities' current state is made, the results are examined and discussed in order to suggest and put into practice improvements to the oil lubrication system's present state.

After the diagnosis was made, a few anomalies were discovered, most notably in the system for distributing oil because several bombs fail to meet the requirements that ensure an excellent bombing of oil along the tubing. Additionally, a minor issue with the refrigerant system was discovered, but which only happens in very rare cases, that is, in situations where the ambient temperature is extremely high, more specifically on extreme summer days, which can be considered insufficient to require intervention. Regarding the filtration system, this is in a similar situation to the cooling system, i.e., it is compatible with most of the daily situations. In very isolated situations, it doesn't have the capacity to correspond to what is required, slightly disturbing the quality of production. However, the investment to solve this problem is too large and without significant improvements in production to be considered worthwhile.

The implementation of potential solutions for the discovered problems followed, including, for instance, replacing the old piping with new piping that had better characteristics and the acquisition of new bombs to replace some of the current ones that couldn’t deliver oil at the right pressure and flow rate.

Resumo

O aumento da taxa de produção e, simultaneamente, a diminuição do custo de produção é a meta de qualquer indústria em todo o mundo. A retificação, também conhecido por *Grinding*, é um dos processos de maquinagem mais utilizado para obter bons acabamentos superficiais e excelentes precisões dimensionais nas ferramentas produzidas. Além disso, inevitavelmente, utiliza fluidos de corte para arrefecer e lubrificar as ferramentas em produção de forma a ser possível atingir a qualidade pretendida e também proteger a peça de trabalho e a ferramenta de corte ou rebolo. No entanto, isto só é viável se estiverem reunidos todos os requisitos para o fluído, neste caso óleo, chegar nas melhores condições às máquinas de trabalho.

O presente trabalho foi elaborado com o objetivo de otimizar o processo de lubrificação nas máquinas de Grinding permitindo, desta forma, melhorar a eficiência de produção e, ao mesmo tempo, procurar reduzir os custos envolvidos no processo, tornando-o mais sustentável em termos ambientais e económicos.

Esta dissertação desenvolveu-se em contexto real, associado a uma empresa de fabrico de ferramentas de corte que disponibilizou as suas instalações a fim de aperfeiçoar estes parâmetros.

Nos primeiros capítulos, é feita uma descrição teórica acerca do processo de Grinding e a importância da lubrificação neste método de fabrico. Adicionalmente, são abordados os conceitos envolvidos em todo o processo de lubrificação, ou seja, desde o sistema de distribuição do óleo através das tubagens, o sistema de filtragem e, por fim, o sistema de arrefecimento. Nos capítulos seguintes, são retratados os equipamentos e aparelhos envolvidos no projeto, é realizado um diagnóstico à situação atual das instalações e, a partir daí, são analisados e discutidos os resultados obtidos com intuito de propor e implementar melhorias em relação à situação atual do sistema de lubrificação de óleo.

Após a realização do diagnóstico, foram detetadas algumas anomalias, principalmente, no sistema de distribuição de óleo, já que diversas bombas não cumprem os requisitos que garantem um ótimo bombeamento do óleo ao longo das tubagens. Também foi identificado um pequeno problema relacionado com o sistema de arrefecimento, mas que apenas acontece em casos muito raros, ou seja, em situações em que a temperatura ambiente se encontra bastante elevada, mais especificamente nos dias extremos de verão, o que pode ser considerado insuficiente para necessitar de intervenção. Relativamente ao sistema de filtração, este encontra-se numa situação semelhante ao sistema de arrefecimento, isto é, apresenta-se compatível com grande parte das situações do dia-a-dia. Em situações muito pontuais, este não tem capacidade de corresponder ao requisitado perturbando ligeiramente a qualidade da produção. No entanto, o investimento para solucionar este problema é bastante avultado e sem grandes melhorias significativas na produção para ser considerado compensatório.

Procedeu-se, seguidamente, à implementação de possíveis soluções para as contrariedades encontradas como, por exemplo, a substituição da tubagem atual por uma nova com caraterísticas mais favoráveis e também à aquisição de novas bombas, capazes de debitar óleo com a pressão e caudal ideal em substituição das atuais.

Ackowledgements

First of all, I would like to express my gratitude to Frezite for providing their facilities and indispensable equipment inherent to the practical work. To the engineers Diogo Costa and André Leite for having played a very active role throughout these months of internship providing an overview of the dynamics of work involving the industrial context. To all its collaborators who were always available to help, especially engineers Marcos Nascimento and Ana Ferreira and also to my colleagues João Brandão, Lara Palha and João Sampaio who were part of the day to day work and also always ready to help.

I would also like to thank my supervisor professor Abel Rouboa for the orientations and support given throughout this project.

Finally, I must thank my parents, my sister and grandmother, and my friends for always supporting and encouraging me throughout this journey.

Contents

List of figures

List of tables

List of abbreviations and acronyms

BEP	Best Efficiency Point
EER	Energy Efficiency Ratio
MQL	Minimum Quantity Lubrication
NPSH	Net Positive Suction Head
TPEC	Total Primary Energy Consumption

1. Introduction

1.1. Relevance

The present dissertation was written in response to a Frezite project, which aimed to analyze the lubrication process in grinding machines in order to evaluate and improve the efficiency of the annual oil consumption. This study also intends to optimize energy efficiency in the industrial sector, which naturally leads to the improvement of the company's economic situation, but also to the reduction of environmental impact.

1.2. Frezite presentation

Frezite is a solution engineering company for cutting tools with applications in the woodworking, plastics, composites and metals industries. The Frezite Group was founded in 1978 and has a vast experience in the design, production, development and marketing of chipping tools.

Currently, it has four major business areas (Wood, Metal, Industrial Machining and Space), factories in Trofa, Vila do Conde and Porto, and six cross-border branches (Spain, Germany, Poland, Czech Republic, Brazil and Mexico). Its technology is distributed in more than 70 countries, and its product portfolio positions its customers in markets as vast and varied as: automotive, food, aerospace applications, sustainable homes, and even aviation. Recently, it was acquired by the Swedish multinational company Sandvik.

1.3. Objectives

In a sector of activity such as the manufacturing industries, framed in increasingly competitive markets, there is a constant need to optimize its production factors. The implementation of the best strategies creates competitive advantages among companies where, for example, the intensive consumption of energy, materials and fluids is considered a fundamental and permanent issue.

The main objective of this dissertation is the study and development of the impact of the optimal condition of lubrication in grinding machines in order to guarantee a more competitive performance. The improvement of this parameter interferes positively in the manufacturing process of the cutting tools.

The realization of this dissertation requires a preliminary evaluation of the state of the art of the equipment. In the initial phase, a diagnosis of the condition of the filtration system and associated pumps, the connecting piping and, finally, the cooling system was performed. This comprises a quantitative and qualitative evaluation of the various equipment integrated into the plant.

1.4. Method followed in the project

The dissertation was developed essentially in Frezite's facilities, in Trofa, more specifically in the metals factory, with the work beginning in September 2022. This month began with the presentation of the facilities and equipment used, as well as contact with the various employees. In that same month and throughout the dissertation, extensive research was carried out in order to acquire the theoretical knowledge necessary for the development of the theme.

At the start of the month of October, field analyses were made, obtaining information about the characteristics of the machines, the physical and thermodynamic properties of the oil used in the company, the piping distribution network, and understanding how the oil was sent and returned between the main tank and the machines. In addition, a survey was also made of the characteristics associated with the filtration process installed in the oil tank, as well as the cooling system implemented.

With the beginning of November, in a first phase, the data obtained was analyzed and searched for possible improvements that could be implemented in a theoretical way. In a second phase and already in December, it was intended to put the investigated measures into practice. In January, a monitoring of the implemented measures was done.

1.5. Thesis structure

This dissertation is divided into 5 chapters. In the first chapter (Introduction) a short introduction is given to frame what will be studied and to define the objectives of the work.

In the second chapter (Bibliographical Review) a search and bibliographical review is made where the fundamental theoretical concepts related to the work developed in this dissertation are described. This chapter begins with an introduction to the basic concepts of machining, focusing fundamentally on grinding. Next, the importance of lubrication in the process is studied. Finally, the basics of the pumping system, the filtration system and the cooling system are presented.

The third chapter (Materials and Methods) gives a description of the equipment and machines utilized and the methods that were used to prepare and elaborate the diagnosis of the current equipment.

The fourth chapter (Results and Discussion) presents the values obtained from the diagnosis performed on the equipment in the plant. Next, proposals are made in order to improve the current problems and increase production efficiency.

The fifth chapter (Conclusion and Proposal for Future Work) presents the main conclusions that were drawn after the analysis of the results, monitoring of some measures that have already been implemented and proposals for future work are made.

2. Bibliographic Review

2.1. Grinding

Grinding is an effective method of removing material by chip removal for hard metals that require a high level of surface finish quality and dimensional accuracy of a workpiece. This means it is crucial to achieve the tight tolerance levels in the established dimensions (R. Rekha 2022). Figure 1 shows a workpiece ready to be machined on one of the factory's machines.

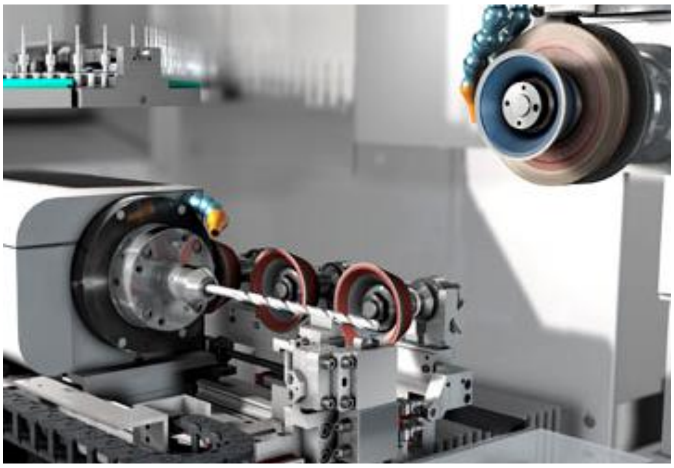

Figure 1- Workpiece positioned to be worked.

In this process, the cutting tool comes in direct contact with the workpiece, inherently leading to effective removal of material, also known as chip (Saroj Kumar Patra 2022). This manufacturing process has associated various input operating parameters such as wheel/cutting speed, cross feed, feed rate and coolant that strongly influence and determine the output parameters, such as, surface roughness, metal removal rate, wear/durability of the cutting tool/grinding wheel, surface and subsurface integrity, dimensional and shape accuracy, thermodynamics, dynamics, among others (Qingyu MENG 2022).

The grinding method plays a key role among all processes (Saikat Chatterjee 2018). According to the survey and represented in figure 2, grinding is considered the most important technology with 25% share, followed by 23% by turning, 22% by milling, 22% drilling and 8% others. Overall, of the total distribution of machines installed in factories, 43% are grinding machines only (H.K. Tönshoff 1998).

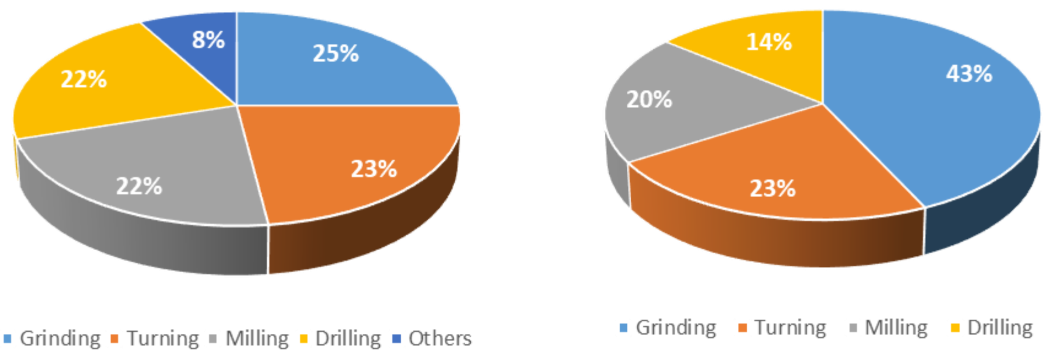

Figure 2- Machining methods practiced in Industry: Share of different machining processes (left); Type of available machines for machining (right) (H.K. Tönshoff 1998).

2.2. Lubricants

Grinding is a process where dimensions and accuracy of workpiece shape, as well as surface quality, are fundamental. As a result, high temperatures have a negative impact on these settings and should be avoided at all costs (Saroj Kumar Patra 2022). Figure 3 represents the main sources and source area of heat during machining (Şenol Şirin 2021).

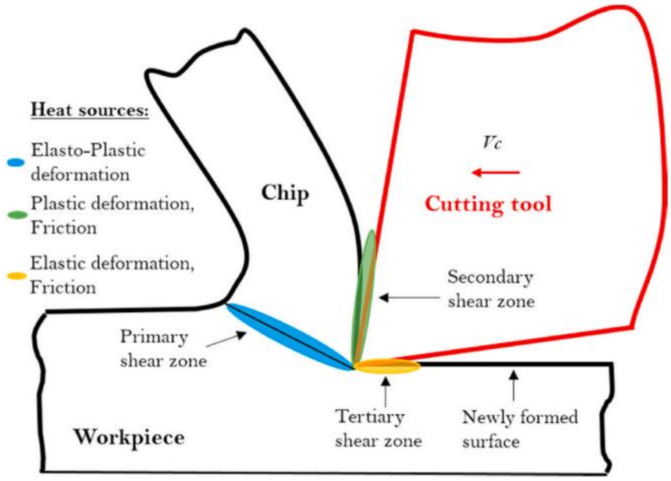

Figure 3- Prime Sources and area of heat generation in machining (Şenol Şirin 2021).

The heat generated due to elasto-plastic deformation is localized in the primary shear zone, while friction and plastic deformation is situated in the secondary shear zone. As for the tertiary shear zone, heat results from elastic deformation and friction (Şenol Şirin 2021).

Heat generation in the grinding zone is greater than much of the other processes, due to the high specific shear energy (M. Bhuyan 2018). During this process, the estimated temperature at the cutting tool edge, chip and the workpiece are 900 °C, 500 °C and 200 °C, respectively. About 25% of the heat generated is due to friction between the chip and tool face while the remaining 75% of the heat is generated due to metal deformation (Mohamed Osama 2017).

Cutting fluids present a series of advantages in machining processes since they are mainly responsible for the heat transfer of the primary and secondary heat zone, i.e., for temperature reduction and lubrication (Pei Yan 2015).

The main factors that make the use of cutting fluids extremely important as a lubricant are (FUCHS SCHMIERSTOFFE GMBH 2017):

- Reduce the coefficient of friction between the tool and the workpiece.
- Expel the chips or metal filings from the cutting zone.
- Protect the tool, workpiece and machine from corrosion and oxidation.
- Cool the tool.
- Cool the workpiece.

In addition, this decrease of heat from the grinding zone is one of the ways to extend the life of grinding wheels and increase efficiency in manufacturing/process by improving the quality of the parts produced by achieving a better finish (Lin 2011).

However, lubricants can also present serious drawbacks related to environmental impacts and high economic costs. Cutting fluids sometimes contain preservatives and pesticides that have serious effects and put the operator's health at risk (Broomer 2000).

The effectiveness obtained in any grinding process depends not only on the chemical and physical properties of the lubricating oil but also on the correct lubrication of the work zone promoting efficient heat extraction (T. Tawakoli 2010).

For heat removal there are different forms of cooling and lubrication, such as: dry machining, flood cooling, cold air cooling and minimum quantity lubrication (MQL) (Saroj Kumar Patra 2022). The pressure of the injected fluid and the speed of the grinding wheel have a great impact on the quality of the machined surface (Zishan Ding 2021). The cooling system used in the factory is flooded type cooling as shown in figure 4. This system brings good results without compromising the parts involved.

Figure 4- Flooded lubrication while the workpiece is being manufactured.

In a study, it is found that in 2019 the value of the global industrial lubricants market was €55.29 billion. The demand for industrial lubricants was estimated to reach a value of €74.64 billion by 2027 with an annual growth rate of 4.8% (Precedence Research 2020). The lubricants industry can be categorized in different ways depending on its application such as motor oils, hydraulic lubricants, gear oils, cutting fluids, and others (Saroj Kumar Patra 2022). In machining, the cooling and lubrication cost is in the range of 7% to 17% of the total production cost, while the tool cost is only 4% (Navneet Khanna 2022).

2.3. Oil pump system

Machines, when they are in operation, inevitably need lubricant. Therefore, it is essential to ensure that there is a good oil distribution system for all machines. For this to be possible, it is mandatory to carry out a good dimensioning of the installation, composed by the pump and the pipes.

Pumps are hydraulic operating machines that impart energy to fluid for the purpose of carrying it from one point to another under process conditions. They receive energy from some motor source and impart some of that energy to the fluid in the form of pressure energy, kinetic energy, or both. In other words, they increase the pressure of the liquid, the velocity, or both (Edson Ezequiel de Mattos 1998).

The most used pumps in industry are centrifugal pumps. Centrifugal pumps stand out for their high efficiency and low installation, operation, and maintenance costs, and for this reason are the ones used in this factory (Tsutiya 2006). These pumps, basically consist of a mobile element, called rotor or impeller with blades, and a fixed element, the housing or volute as shown in figure 5.

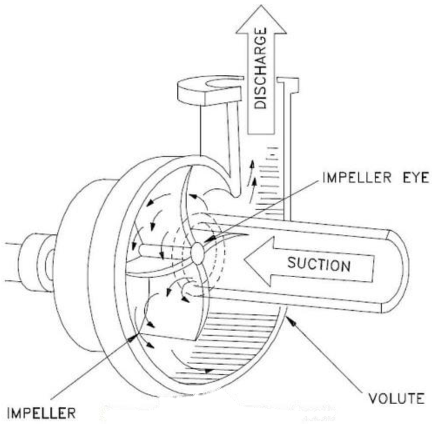

Figure 5- Schematic representation of a centrifugal pump (HardHat Engineer 2022).

The rotor or impeller rotates inside the housing, and its movement produces a vacuum zone (center) and a high pressure zone (periphery). The fluid enters the center of the impeller because of this vacuum and is accelerated by the blades that rotate at high speed. By the action of centrifugal force, the fluid is discharged into the volute or diffuser, where it is decelerated by an expansion of the flow section. Thus, the acquired kinetic energy is transformed into pressure energy (Edson Ezequiel de Mattos 1998).

The oil pumping system is defined by different parameters such as energy balance, manometric height, pressure drop, cavitation, Net Positive Suction Head (NPSH) and pump sizing.

2.3.1. Energy Balance and Manometric Head

The fluid flow along the entire pipe can be considered permanent uniform, therefore it is practical to use Bernoulli's equations (conservation of energy) and continuity to calculate the manometric head (Edson Ezequiel de Mattos 1998). Bernoulli's equation, which describes the energy balance between the reservoir (left side of equation) and the machine (right side of equation), has been slightly modified by adding the pump's work and pressure drops as shown in equation (1):

$$\frac{P_r}{\gamma} + \frac{V_r^2}{2g} + Z_r + h_a = \frac{P_M}{\gamma} + \frac{V_M^2}{2g} + Z_M + h_L \quad (1)$$

Where,

$\frac{P}{\gamma}$ = piezometric pressure height (m).
$\frac{V^2}{2g}$ = kinetic velocity (m/s).
Z = static height (m).
h_a = energy delivered per unit weight to the liquid by the pump (m).
h_L = total head loss (m).

The energy balance between the convenient points must be applied to calculate the manometric height of the installation, which is the sum of the geometric height of the installation and the head losses along the flow path. The manometric height is described by the equation (2):

$$H_m = H_G + h_L \tag{2}$$

Where,

H_m = manometric height of the installation (m).
H_G = geometric height (m).

Physically, it is the amount of energy that the pump must provide to move the oil at a given speed from the reservoir to the machine, through the pipes of defined diameters, overcoming the geometric unevenness and the resistances in the form of pressure drop (Carlos Rogério de Mello 2010). The geometric height is the difference in height between the liquid surface in the container above and the liquid surface in the container below. In addition, the pumps can be vertical or horizontal axis pumps as well as positive or negative suction pumps depending on their position relative to the tank. Figure 6 provides a simple schematic illustration to demonstrate examples of pump classifications.

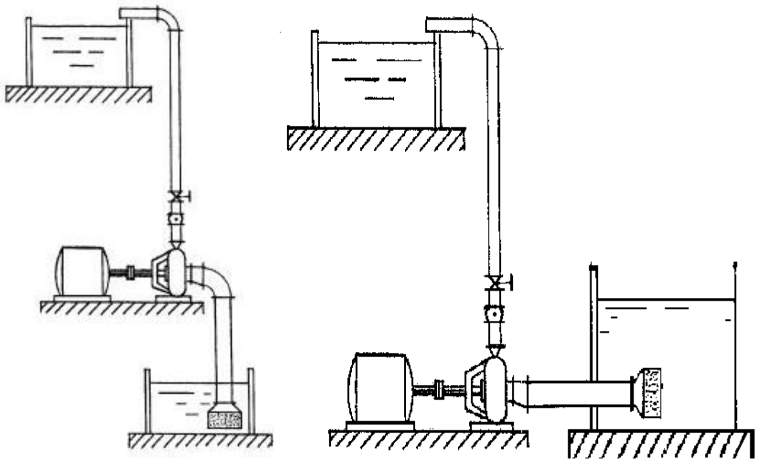

Figure 6- Classification of pumps in relation to shaft position: a) positive and vertical suction; b) negative and horizontal suction (Carlos Rogério de Mello 2010).

2.3.2. Pressure Drop

The pressure loss, or energy loss, refers to the energy lost by the oil on its way through the pipe. This energy loss results from the liquid's internal friction, or viscosity, as well as the resistance provided by the oil to the pipe walls due to their roughness. The roughness values considered are shown in Appendix A (White 2016).

In addition, the changes in trajectory/direction caused by the interconnections of the piping and the turbulence that causes a change in velocity are factors that contribute to the load losses. Therefore, when designing the pumping system, it is crucial to consider this loss of mechanical energy that is dissipated in the form of heat.

Thus, the calculation of the total pressure drop will be divided into two parts, the in-line pressure drop of constant circular cross section (distributed) and head loss at pipe accidents (localized), as shown in equation (3):

$$h_L = h_{L\,Line} + h_{L\,Local} \tag{3}$$

Where,

$h_{L\,Line}$ = Head loss line (m).
$h_{L\,Local}$ = Head loss local (m).

Once the total pressure drop is defined, we naturally have the manometric head.

Next, each of the parts involved in the total pressure drop will be presented:

1) In-line pressure losses: These are those associated with losses along the pipe, and are a function of length, material, and diameter.

The equation (4), often known as the universal or rational formula, is used to calculate the in-line pressure losses and is valid for any liquid:

$$h_{L\,Line} = f\frac{L}{D}\frac{V^2}{2g} \tag{4}$$

Where,

f = Darcy's friction factor or resistance factor.
L = Length of pipe (m).
V = Average velocity of the fluid (m/s).
D = Internal diameter of the pipe (m).
g = Acceleration constant of gravity (m/s^2).

Equation (4) can also be transformed and be expressed as follows in equation (5):

$$\Delta P = f\frac{L}{D}\frac{\rho V^2}{2} \tag{5}$$

Where,

ΔP = Pressure drop (Pa).
ρ = Specific mass or absolute density (Kg/m^3).

The type of flow also influences the pressure drop process. The flow regime can be turbulent, transient, or laminar as shown in figure 7.

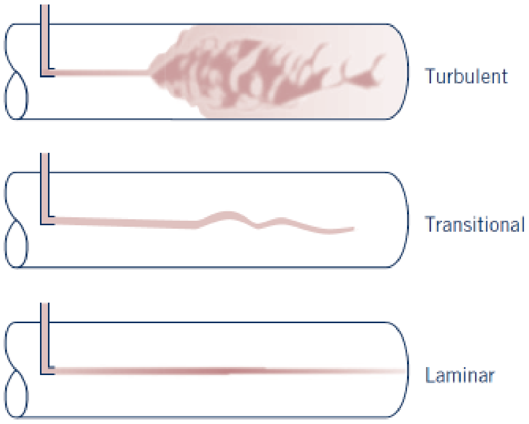

Figure 7- Types of flow regimes (Philip M. Gerhart 2016).

The Reynolds number (Re), which is calculated in equation (6), is the parameter that determines which of the regimes the fluid is in:

$$Re = \frac{DV\rho}{\mu} = \frac{DV}{v} = \frac{4 \times Q}{\pi \times D \times v} \quad (6)$$

Where,

Re = Dimensionless Reynolds number.
μ = Dynamic viscosity (Kg/m.s);
v = Kinematic viscosity (m^2/s).

The regime is considered laminar for Reynolds values below 2100. The transient regime is associated for values between the range 2100 < Re < 4000. For values above 4000, the regime is assumed to be turbulent (Philip M. Gerhart 2016).

To estimate the value of the friction factor (f) there are several correlations, of which we can mention: Moody Diagram and Colebrook equation.

The Moody Diagram, shown in figure 8, is one of the methods for calculating the friction factor. The Moody chart is universally valid for all steady, fully developed, incompressible pipe flows. This quick and relatively accurate solution is a log-log diagram where, by entering the Reynolds number (Re) value on the abscissa (x-axis) and the relative roughness (ε/D) on the right ordinate (y-axis), you get the friction factor (f) on the left ordinate by correlation [22]. For laminar flow, f = 64/Re, which is independent of relative roughness. For turbulent flows with very large Reynolds numbers, f is independent of the Reynolds number. For flows with moderate values of Re (transient regime), the friction factor is indeed dependent on both the Reynolds number and relative roughness.

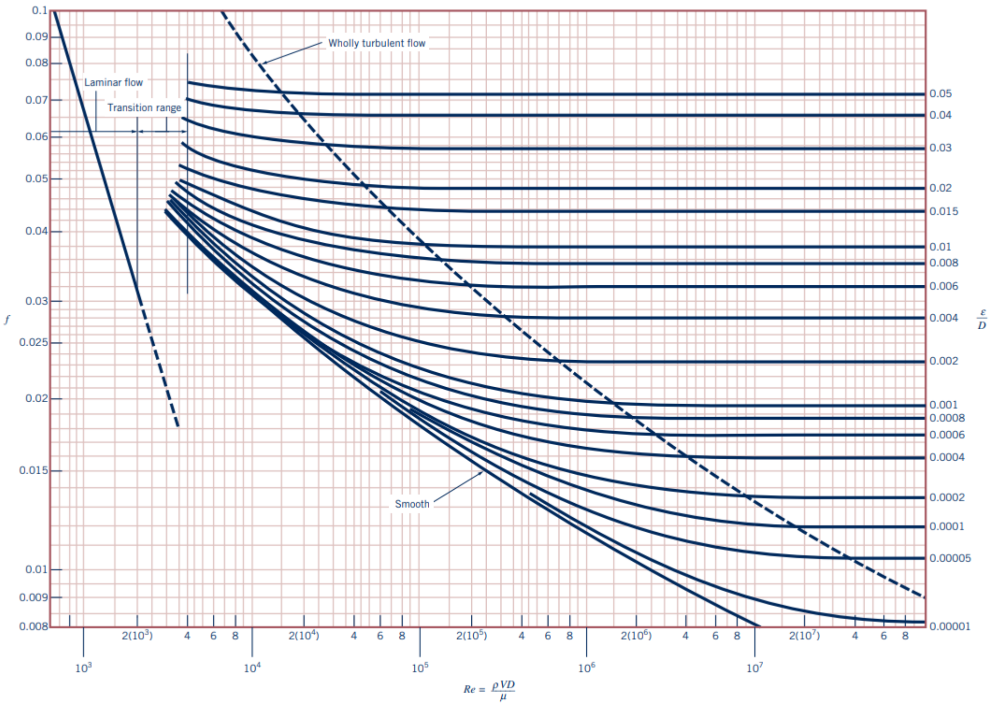

Figure 8- Friction factor as a function of Reynolds number and relative roughness for pipes -Moody chart (Philip M. Gerhart 2016).

The Colebrook equation (7) is the most accurate correlation to estimate the value of f although it is implicit. This equation is valid for smooth and rough pipes in the fully developed transition and turbulent regimes (White 2016).

$$\frac{1}{\sqrt{f}} = -2{,}0 \log\left(\frac{\varepsilon/D}{3{,}7065D} + \frac{2{,}5226}{Re\sqrt{f}}\right) \tag{7}$$

Where,

ε/D = relative roughness.

2) Local or accidental pressure losses: These are those provided by elements that make up the pipe, that is, they are losses of energy observed in accessories such as bends, valves, branches, bifurcations, connections, contractions, and expansions. The loss coefficients caused by the components of the pipe are displayed in Annex A [20].

The localized pressure losses can be expressed by the equation (8) in the form:

$$h_{L\,Local} = K\frac{V^2}{2g} \tag{8}$$

Where,

$h_{L\,Local}$ = Head loss local (m.f.c.).
K = Head loss coefficient (dimensionless).

2.3.3. Cavitation and NPSH

Cavitation is a phenomenon in which the liquid reaches pressure below atmospheric pressure (P_{atm}), such that it becomes lower than its vapor pressure (H_v). The liquid boils at room temperature and turns into vapor. It then receives an energy boost from the rotor blades and the pressure becomes higher than P_{atm}. The figure 9 schematically shows how the cavitation phenomenon arises.

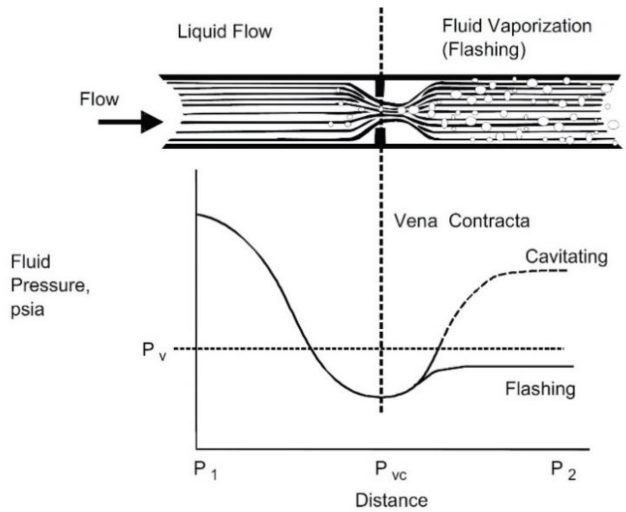

Figure 9- The cavitation process in pipelines.

In this situation, explosions of short duration but great intensity occur. This effect causes corrosion of the metal particles in the pumping cavity and the rotor causing damage, mainly to the rotor and blades and being identified by noise and vibrations. To avoid this phenomenon, the required NPSH and the available NPSH should be analyzed.

The NPSH available refers to the availability of energy with which the liquid enters the pump to allow the suction of the fluid, that is, it depends on the local conditions and on the characteristics of the pump installation. This NPSH must be studied by the plant designer, using the expression (9):

$$NPSH_{available} = \frac{Patm\ local}{\gamma} - (\pm Z_{suction} + H_V + H_{L\ suction}) \tag{9}$$

Where,

$NPSH_{available}$ = available energy at the facility for suction (m).

$\frac{Patm\ local}{\gamma} = H_{atm}$ = local atmospheric pressure- Annex C (José Martiniano de Azevedo Netto 2015).

$Z_{suction}$ = suction height; it is negative when the pump is drowned, and positive when it is above the water level (m).

H_V = vapor pressure of the fluid as a function of its temperature- Annex C (M. 2014).

$H_{L\ suction}$ = total pressure drop in the suction line (m).

The NPSH required is the net energy load required by the pump to promote suction, with its pressure value necessarily higher than vaporization, that is, it is the energy that must be available inside the pump to avoid the cavitation phenomenon. This parameter is provided, graphically as a function of flow, by the manufacturer together with the pump curves.

It is therefore observed that the energy available in the installation for suction must be greater than the energy required by the pump, that is, $NPSH_{available} \geq NPSH_{required}$. If this occurs, the pump meets the operational requirements and theoretically can be used in the design. Otherwise, cavitation will occur because of poor suction. In such situations, other pump options should be analyzed, regardless of the supplier, in order to avoid the cavitation phenomenon.

2.3.4. Pump sizing

As seen before, the rotor blades cause the fluid to accelerate, transforming mechanical energy into kinetic energy. The rotation of the rotor blades, their shape, and their size influence the intensity of the energy delivered to the fluid. Thus, the characteristic curve of the pump changes according to these parameters. For a given motor with a rotor of defined diameter and shape and constant speed, the pump curve does not change and is almost independent of the liquid being pumped (Edson Ezequiel de Mattos 1998).

Figure 10 shows a pre-selection chart of pumps of the brand used by the company, from which the customer has an idea of which catalogs to consult regarding the selection itself, locating the working point in this graphic and determining which is the ideal pump.

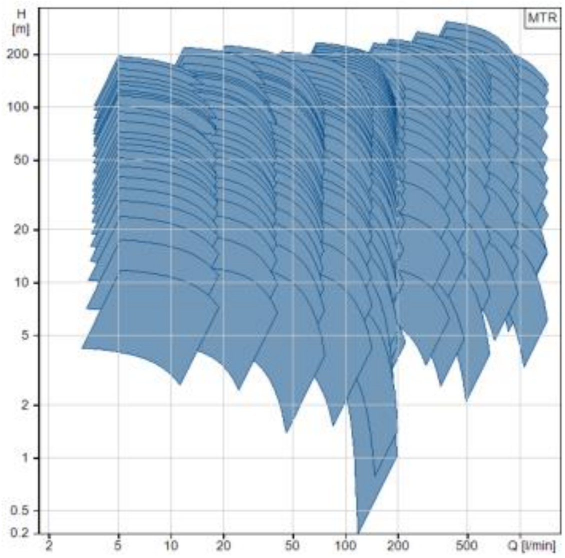

Figure 10- Representation of a pump pre-selection chart (Grundfos 2022).

The characteristic curves graphically defined by the manufacturer show as variables: the head (H_m), the efficiency (η) and the $NPSH_{required}$ as a function of the flow rate. Pump performance characteristics from pump manufacturers are presented in charts of the type shown in figure 11. These three variables characterize the operating conditions of a specific pump.

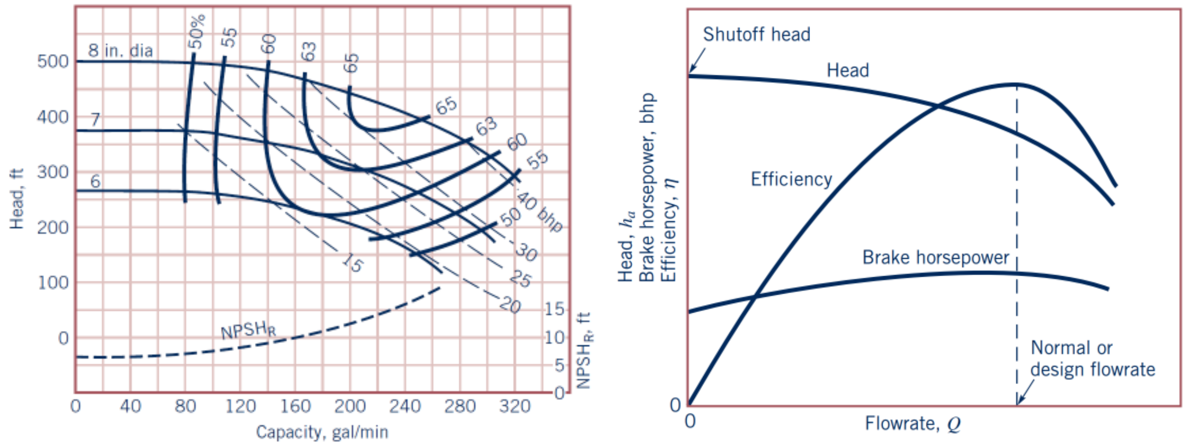

Figure 11- Characteristic curves of pumps [20].

Using the manufacturer's catalog of pumps, the intention is to choose the most suitable pump for the system, and this should be done so that the pump operates at or near the point of maximum efficiency. Otherwise, its useful life and operating conditions will be impaired.

Equation (10) is the mechanical energy equation applied in a typical flow system in which a pump is used is:

$$h_a = \frac{P_2 - P_1}{\gamma} + Z_2 - Z_1 + h_L \tag{10}$$

Where,

h_a = Actual head supplied by the pump (m).

h_L = All friction losses in the pipe and minor losses for pipe fittings and valves (m).

However, according to the study of flow in pipes, h_L can vary approximately as the squared flow rate, that is, $h_L \propto Q^2$. Equation (11) is the system equation and shows how the actual head gained by the fluid from the pump is related to the system parameters (Philip M. Gerhart 2016).

$$h_a = \frac{P_2 - P_1}{\gamma} + Z_2 - Z_1 + KQ^2 \tag{11}$$

Where,

K = Friction factors and head loss coefficients (m).

Q^2 = Flow rate (m^3/s)

In the case of the equation (11) the system parameters include the change in elevation head, $\frac{P_2-P_1}{\gamma} + Z_2 - Z_1$, and the losses due to friction as expressed by KQ^2. Each flow system has its own specific system equation (Philip M. Gerhart 2016).

The system curve, also known as the pipe curve, is a curve plotted on the H_a x Q graph as the example shown in figure 12.

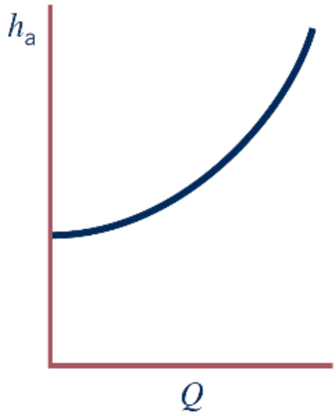

Figure 12- Diagram of a system curve.

To determine the operating point when a specific pump is installed in a specific system, it is necessary to utilize both the system curve, as determined by the system equation, and the pump performance curve. If both curves are plotted on the same graph, as illustrated in figure 13, their intersection (point A) represents the operating point for the system. That is, this point gives the head and flow rate that satisfy both the system equation and the pump equation.

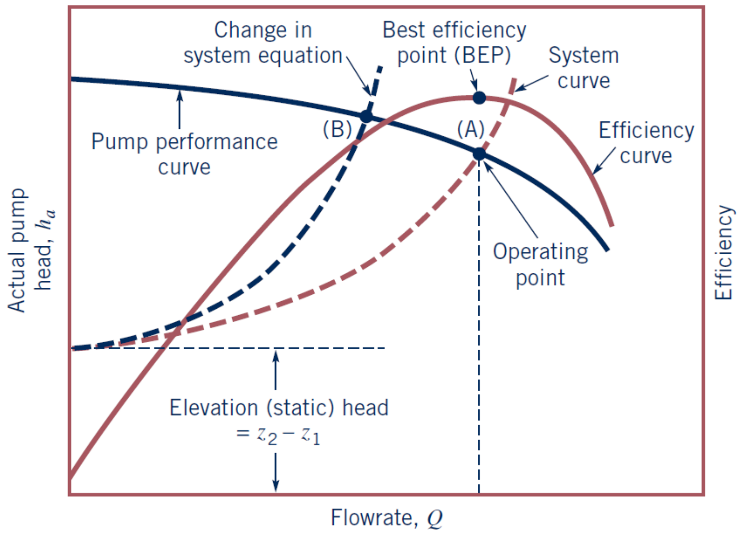

Figure 13- Utilization of the system curve and the pump performance curve to obtain the operating point for the system (Philip M. Gerhart 2016).

On the same graph the pump efficiency is shown. Ideally, we want the operating point to be near the best efficiency point (BEP) for the pump. For a given pump, it is obvious that as the system equation changes, the operating point will shift. For example, if the pipe friction increases due to pipe wall fouling, the system curve changes, resulting in the operating point A shifting to point B in figure 13 with a reduction in flowrate and efficiency.

2.4. Filtration System

The Transor Filter GMBH filtration plant has numerous applications.

Oil, contaminated by the particles released by the grinding process, flows from the grinding machines into the contaminated oil sump of the filter system via the return line. A pump transports the dirty oil through the lower cylindrical part of the filter towers and passes it through the filter rods to the top of the filter tower. Impurities larger than 3 µm are removed during filtration by sticking to the surface of the filter rods. Figure 14 gives an idea of the filtration range that the system installed in the plant is capable of. The cleaned and purified oil exits the filter towers at the top through a pneumatically operated hydraulic valve and goes into the clean oil tank.

The contaminated oil tank naturally receives the oil coming from the machines through the return pipes, but also admits oil when regeneration is carried out to the filter rods. This happens periodically and when the filter towers are emptied, their contents quickly pass into the contaminated oil tank.

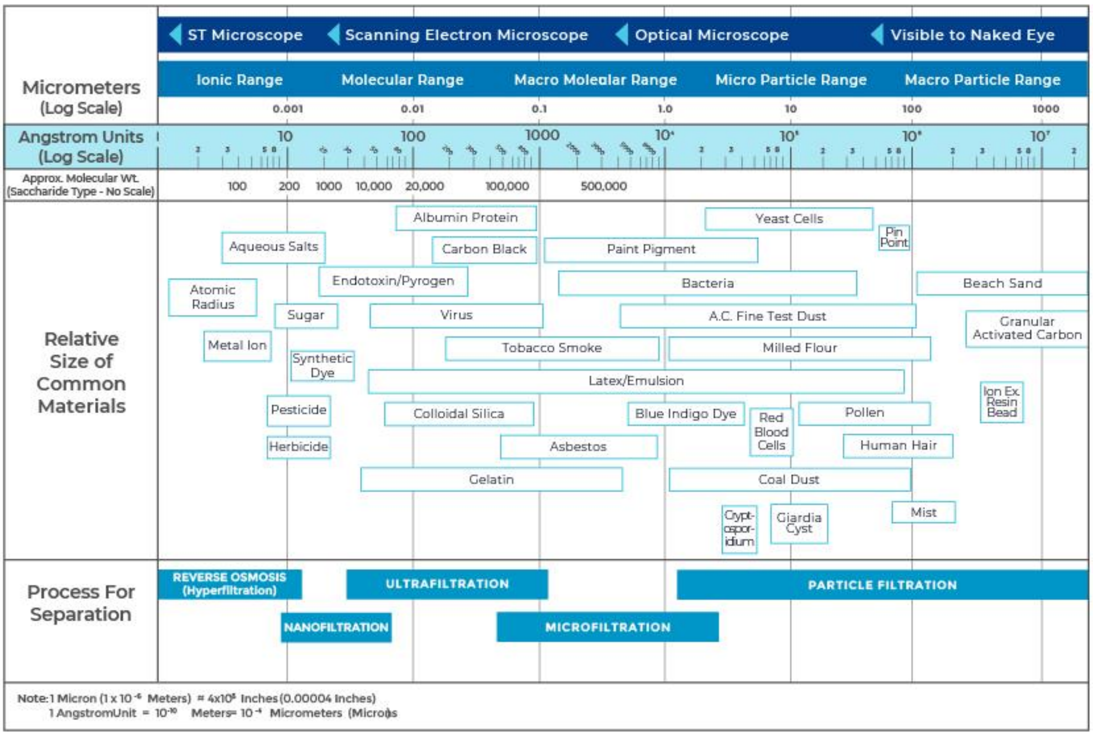

Figure 14- Particle spectrum and separation processes.

As for the clean oil tank, this is used to supply clean oil back to the working machines. This tank is necessary as the filter towers need to occasionally regenerate and clean themselves after a certain number of operating hours. The clean oil reservoir has the function of ensuring that the machines are supplied without interruption even during the brief periods when filtration is interrupted. The figure 15 schematically represents the filtration system described above.

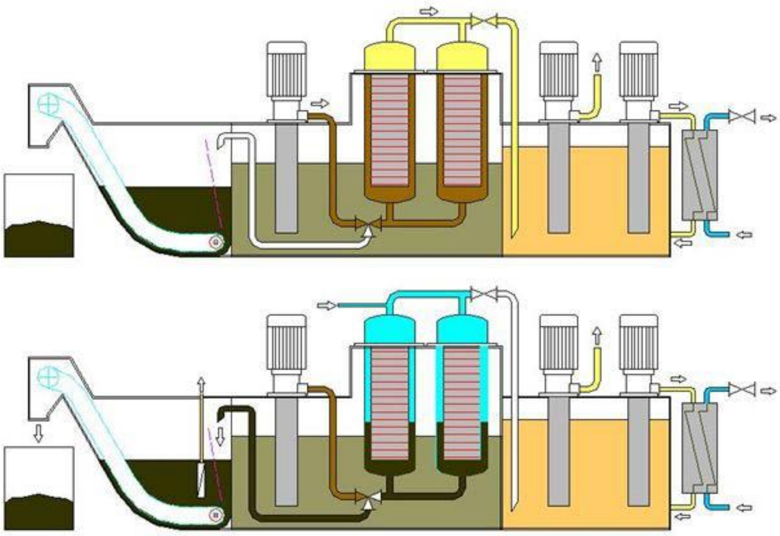

Figure 15- Representation of Filtration system.

Oil treatment with a Transor filtering system offers the following advantages:

- Uninterrupted operation of the machines, even during the regeneration time of the filter rods.
- Constant supply of the machines with the same amount of oil and the same oil pressure.
- Reduced disposal costs.
- Significantly lower oil consumption.
- Automatic regeneration of filter rods.

2.5. Cooling System

Chillers transfer heat out of a space that is intended to maintain climate control within certain characteristics favorable for proper working operation.

There are two types of chillers: water-cooled and air-cooled. They work similarly throughout most of the process until the refrigerant reaches the condenser. The main difference is that water-cooled chillers use water to surround the cooling tubes and absorb heat in the condenser. The water is then pumped into a cooling tower to release the heat. In the situation with air-cooled chillers, outside air is moved by fans through the condenser, which then transfers heat from the refrigerant to the surrounding air.

Next, the entire air-cooled chiller operation will be described, because this is the method implemented at the facility. The cooling process begins with the primary return from the main reservoir bringing hot oil to the chiller, more specifically to the evaporator, and where heat is transferred from the oil to the coolant.

The now cooled oil is then sent back to the oil reservoir via the primary supply (shown in blue), where it will then be distributed via pumps to the manufacturing machines. Since heat always passes from hot to cold, as indicated by the second law of thermodynamics, the cooled oil absorbs the heat caused by the entire process related to the oil distribution system, especially in the tool manufacturing operation. The warmer oil is then returned to the chiller to be cooled once more. This entire process is schematically shown in Figure 16.

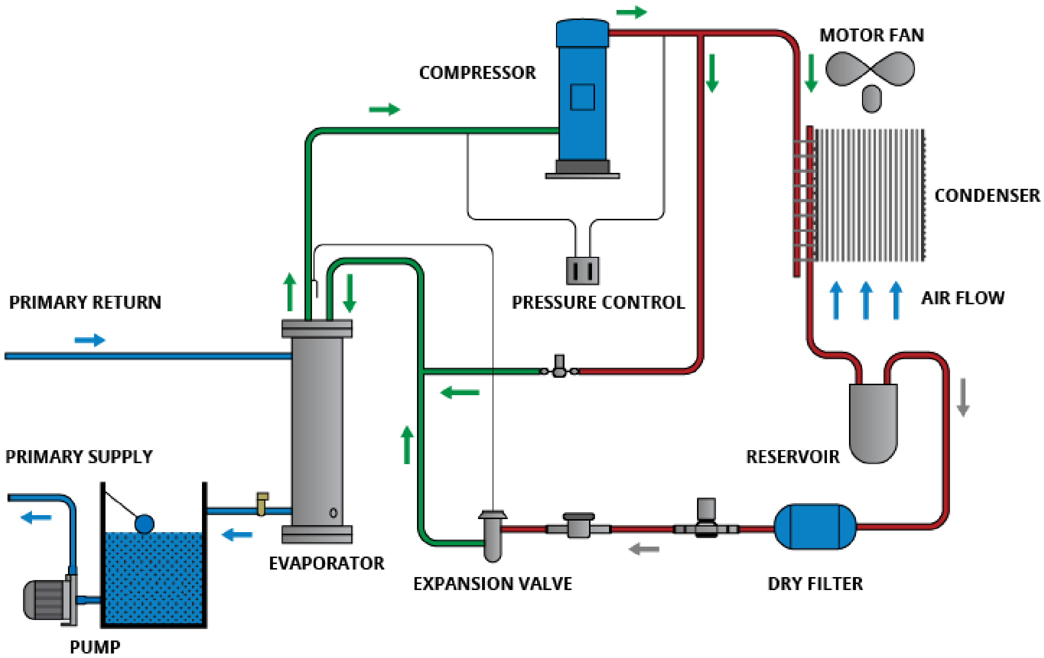

Figure 16- Air-cooled chiller diagram (HVAC Investigators 2022).

Meanwhile, the heat absorbed by the refrigerant (path shown in green) in the evaporator needs to be transferred to allow the refrigerant to absorb more heat. The low pressure, high temperature refrigerant passes from the evaporator to the motor compressor, which raises the pressure and temperature.

After that, the refrigerant enters the condenser. Here, fans circulate outside air through the condenser and absorb heat from the refrigerant before expelling this heat into the ambient air. After condensation, the refrigerant passes through an expansion valve to reduce the pressure and temperature and returns to the evaporator, where the process begins again (HVAC Investigators 2022).

When a tool is being produced and thrown against a grinding machine to lubricate it, heat is naturally exchanged with the oil, raising its temperature. The pumps that supply oil to the machines have an impact on the oil's temperature as well. Additionally, the higher ambient temperature on hot days will affect the oil temperature.

The effectiveness of the chiller is a further important component of the cooling system. The cooling effectiveness of air conditioning systems is referred to the energy efficiency ratio (EER). Therefore, an air conditioning system's EER is 2.93 if it produces 2.93 kW of cooling with 1 kW of supplied electricity. The equipment is more energy efficient the higher the EER.

2.6. Energy

Energy represents a basic need for a variety of purposes and has become essential to the competitiveness and rapid growth of the global economy. The rational use of energy and natural resources is the key to sustainable development. With this development, current society's needs are being met while preserving the capacity of future generations to meet their own needs (Bilgen 2014). Hence the importance of an analysis of the future of energy use in global terms. The decisions are made in the present based on the outlook for energy consumption.

Fossil fuels like coal, oil, and, more recently, natural gas have been used to meet the rising energy demand brought on by the economic, technological, and social development of industrialized countries as shown in figure 17. Due to the global pandemic in 2020, this trend was only occasionally interrupted but quickly returned (Roser 2022).

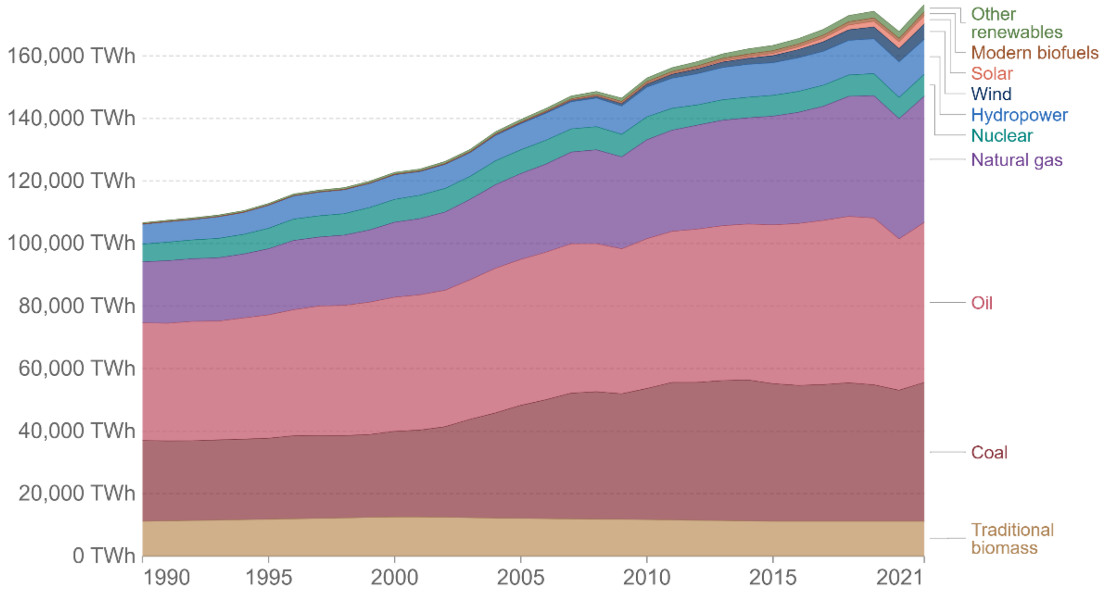

Figure 17- Global Primary Energy consumption by source (Roser 2022) .

Looking at figure 18, Portugal registered in 2020 a Total Primary Energy Consumption (TPEC) of approximately 20 000 ktoe, the lowest value since 2000 when it registered a value close to 25 000 ktoe. Analyzing the consumption of the different forms of energy in 2020, oil continues to be the main source of primary energy source (40.9%), followed by renewables (29.9%), natural gas (25.0%) and coal (2.7%) (Observatório da Energia, DGEG, ADENE 2022).

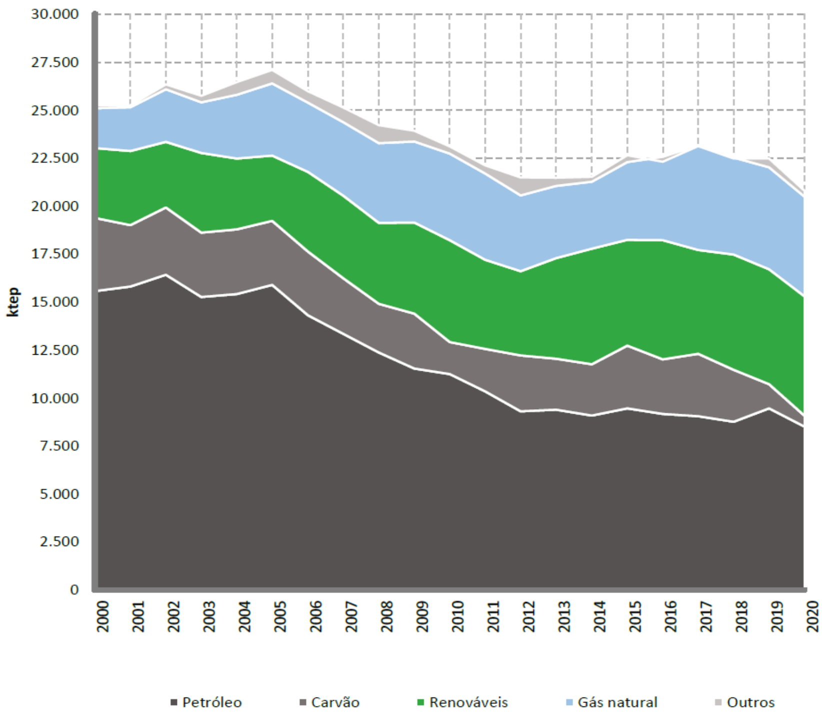

Figure 18 - Evolution of total primary energy consumption in Portugal (Observatório da Energia, DGEG, ADENE 2022).

In 2020, the transport sector remained the main energy consumer (32.6%), followed by industry (31.2%), households (19.5%), services (13.4%) and agriculture and fishing (3.3%), illustrated in figure 19 (Observatório da Energia, DGEG, ADENE 2022). Comparing the years 2020 with 2000, it is evident that the energy spent in transport and industry decreased a little while the other sectors had a slight increase. Focusing exclusively on the industry sector, one notices that in the space of 20 years this sector had a not very significant drop and that it continues to represent about one third of all primary energy. This reveals that this sector is always very present as the years pass by and that it should try to mitigate its consumption by seeking new solutions.

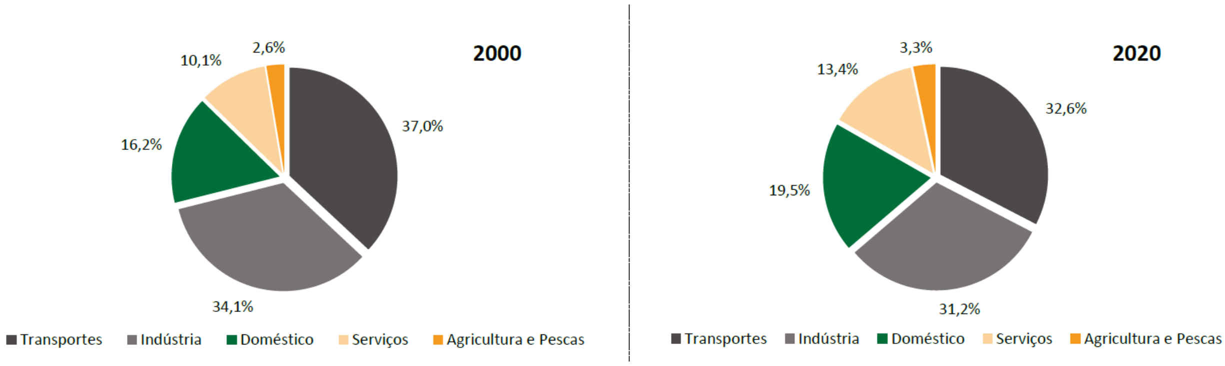

Figure 19 - Total primary energy consumption in 2000 and in 2020 (Observatório da Energia, DGEG, ADENE 2022).

3. Materials and Methods

This section will begin with a brief explanation of the equipment used during the entire process of distributing oil. The techniques utilized to carry out the equipment diagnostics will then be made public.

Naturally, the grinding machine is where the workpiece production process begins. However, the oil's journey begins in the reservoir, as shown in the figure 20. In the installation there are two reservoirs that work in a closed circuit, that is, each one has several machines associated exclusively. However, the mode of operation in each is the same, and so the description that is given of one circuit applies equally to the other. Next, the simplified route of the oil through the manufacturing process will be described.

Figure 20- Oil reservoir.

When machining starts, the pump installed on the reservoir turns on and pumps the oil through the distribution system, i.e., through the pipelines until it reaches the grinding machine. Figure 21 shows an example of an installed pump on top of the reservoir which shows that this pump is installed vertically and above the oil level in the tank. Figure 22 illustrates the pipes (orange) through which the oil passes on its way from the reservoir to the machine and vice versa.

Figure 21- Installed pump above the tank.

Figure 22- Pipelines where the oil circulates.

When the oil reaches the machine, shown in figure 23, it performs its main task, cooling and lubricating the part being worked on, running through the machine and out the bottom of the machine. After leaving the machine, the oil enters a small tank and, using a return pump, is sent back to the main tank through the pipes again. The small reservoir and the return pump are depicted in figure 24.

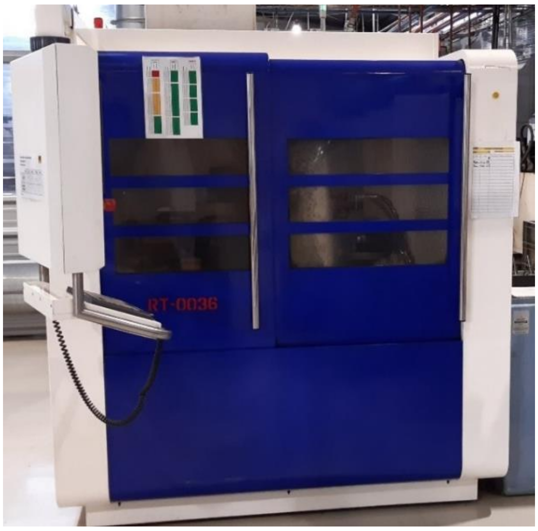

Figure 23- Grinding Machine.

Figure 24- Small tank and return pump.

Returning to the main reservoir, the oil enters the dirty compartment where it is then subjected to the filtration process by passing through the filter towers illustrated in figure 25. After performing the filtration process the oil is placed in the clean oil compartment. Only the cooling system, which is represented by the chiller in figure 26 and connected to the clean compartment of the reservoir, needs to be passed through for the oil cycle to be considered complete. After that, the oil ultimately returns to its original state and is prepared to be released by the pump once more in order to restart the cyclical cycle.

Figure 25- Filter towers.

Figure 26- Chiller.

Once the description of the oil path is finished, we move on to the technical characterization of the equipment used in the factory.

The lubricating oil used in the company is Blasogrind HC 10, illustrated in figure 27. This is a high-performance grinding oil based on synthetic oil. It has excellent physical and chemical properties, of which the most important are:

- Higher flash point and reduced emissions compared to mineral oils.
- Low viscosity, i.e., ν = 10 mm^2/s.
- Density (ρ) = $0.85 g/cm^3$.
- Colorless.
- Good machine compatibility.
- Better surface quality.
- Higher grinding wheel life.

This oil has more characteristics that can be seen in appendix B.

Figure 27- BlasoGrind oil barrel.

The factory features two oil reservoirs that feed a total of 13 machines. The dimensions of the reservoirs are not the same and, therefore, are characterized in table 1:

Table 1- Reservoir characteristics

Reservoir	**1**	**2**
Dimensions (LxWxH) [mm]	3500 x 2000 x 2400	3500 x 2000 x 1600
Total Tank Capacity [l]	3500	2500
Contaminated Tank Capacity [l]	2500	1750
Clean Tank Capacity [l]	1000	750

Figure 28 shows the existing floor plan of the plant area involved in the project. This is a simplified schematic of the piping and machinery distribution. As can be seen, the machines are evenly distributed among the reservoirs, with one reservoir having 7 machines while the other has 6. Naturally, the larger pool is the one with the most machines associated. Concerning the pumps, these are on top of the containers and in total there are 9 pumps to distribute to all the machines. This happens because there is a pump that is connected to 5 machines. It is simpler to evaluate and compare the pumps because they are all from the same manufacturer, *Grundfos*.

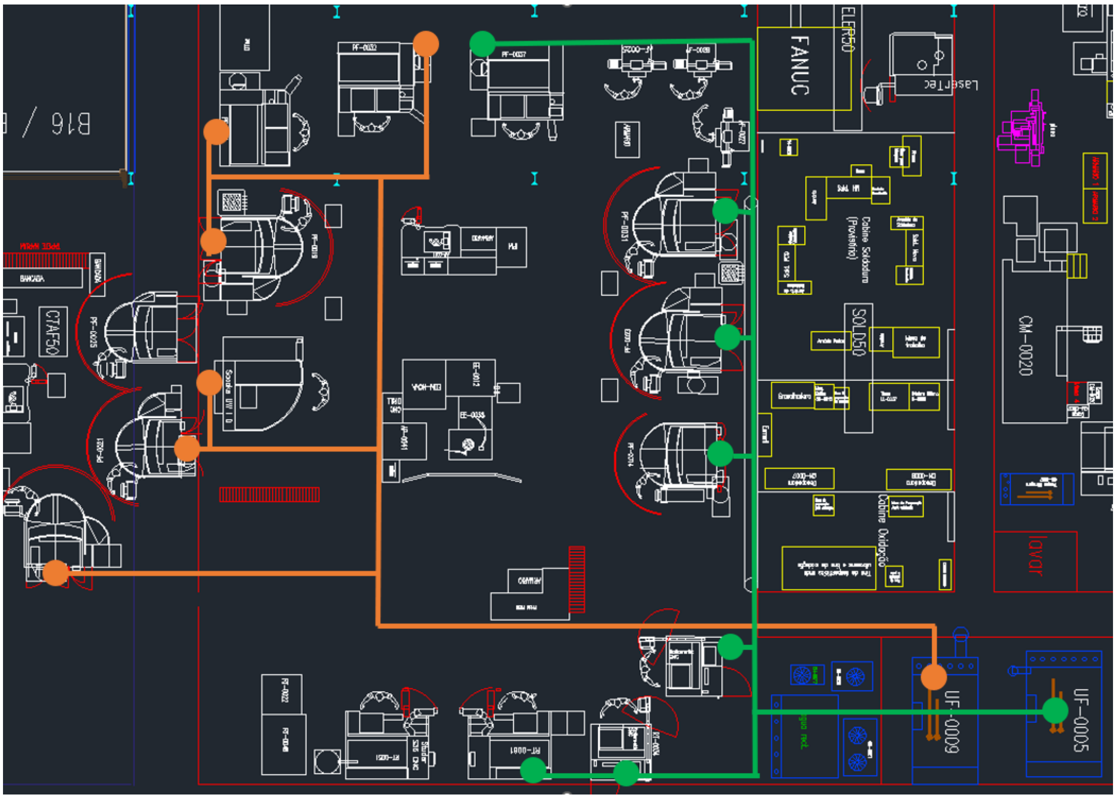

Figure 28- Machinery and pipelines layout.

The pipes in the distribution system have the following features, shown in table 2:

Table 2- Pipe characteristics

Material	Galvanized iron
Maximum Length [m]	45
Diameter [mm/pol]	31.75 / 1.25
Roughness [mm]	0.15

The maximum distance considered in table 2 refers to the machine that is furthest from the reservoir. In this way, the most unfavorable situation is tested. The roughness value was taken from the table 2.

There are several connectors in the piping that connects the tank and the machine that cause a localized pressure decrease. The number of elements employed differs based on where the machine is located, and the pressure drop values also vary. As a result, the most flawed path that runs beside the machine that is most remote from the reservoir was identified. The worst-case scenario is thus verified.

These components are as follows:

- 5 x Elbows long radius 90° threaded.
- 2 x Elbows long radius 45° threaded.
- 5 x Unions threaded.
- Entrance flow loss.
- Exit flow loss.

The 13 machines in the factory are not all from the same supplier. However, the requirements of the machines concerning the oil flow for cooling the workpiece and the pressure at which it is released do not differ between them:

- Oil pressure in the machine = 6 bar.
- Oil flow rate = 120 l/min.

In order to raise production yield, ensure proper machine maintenance, and improve the quality of manufactured parts, it is crucial to meet these requirements. The pressure at the pump outlet and at the machine inlet can be measured by manometers, as exemplified in figure 29, which are installed at these locations. Regarding the required oil flow rate, unfortunately, the plant does not have a flow meter to control and monitor the rate of oil being released by the pumps, and therefore relied on the characteristic curves of the pumps and their capacity to deduce the flow rate being pumped to the machines.

Figure 29- Pressure gauge installed on the pipes.

Regarding the filtration system, there are 4 filtration towers in each reservoir. Each filter is capable of filtering about 100 liters per minute, i.e., in total about 400 liters per minute for each tank.

Additionally, the plant has two chillers with various features that were gleaned from the catalogs in appendix D and summarized in table 3:

Table 3- Chillers characteristics

Chiller	**1**	**2**
Model	EQUIFAB ESE – 022	HITEMA ENR – 022
Power [KW]	22.0	22.5
Flow rate [m^3/h]	3.8	3.8
EER:	2.93	3.4

There are two separate oil distribution circuits, or to put it another way, tank number one has chiller number one and a specific number of machines connected to it. The other circuit experiences the same thing but for the remaining equipment. As a result, even though the oil in each circuit is the same, there is never any mixing between them. In this manner, if a problem arises, it is simpler to identify and does not require a complete shutdown of all machines for repair, allowing production to continue in part. The purpose of the chiller is to cool the oil so that it remains at a temperature of 26°C in the reservoir, ready to be released to the machines. The oil temperature can be controlled through temperature sensors incorporated in the machines as can be seen in figure 30. In addition, the machines integrate a warning system if the oil temperature and the ambient temperature differ by 3°C. Ideally, this value should not be exceeded, but sometimes the ambient temperature in the facility varies greatly in both winter and summer.

Figure 30- Oil temperature control at the machine inlet.

It is time to perform the diagnostic calculations to verify the condition of the equipment in the installation once the primary characteristics of the project's components have been provided.

The following steps should be taken in order to perform the system sizing, in particular, the filtration system:

- Apply the energy balance.
- Define the pipe diameter.
- Calculate the pressure drop.
- Determine the total head.
- Dimension the pump through curves provided by manufacturers and as a function of the parameters previously defined.
- Calculate the NPSH.
- Check the risk of cavitation.

In addition, it is also necessary to analyze the condition of the reservoirs in terms of capacity. Finally, a check is made on the filtration system associated with the reservoir as well as the cooling system.

4. Results and Discussion

In the first part, the calculations and results associated with the current conditions of the equipment operating in the facility are demonstrated. In this situation, the machine that presents the least favorable conditions will be tested, i.e., the one that is furthest from the reservoir and has associated higher losses. In a second phase, improvement proposals will be presented in order to improve conditions and increase production yield.

4.1. Equipment Diagnostics

As mentioned in the previous section, the steps for sizing the oil distribution system were followed, starting with the application of the energy balance present in equation (15). This stage is followed by the calculation of the pressure drop and the determination of the total head. Since the state of the installation is being checked, the diameter is defined. The goal in this step is to understand what value the pump should be able to achieve to meet the pressure and flow requirements demanded by a machine.

$$\frac{P_r}{\gamma} + \frac{V_r^2}{2g} + Z_r + h_p = \frac{P_M}{\gamma} + \frac{V_M^2}{2g} + Z_M + f\frac{l}{D}\frac{V^2}{2g} + \sum K_{L\ Local}\frac{V^2}{2g} \quad (12)$$

A part of the equation's variables takes the value zero simplifying its resolution, as is the case with the oil pressure in the reservoir where it is assumed to be at atmospheric pressure ($P_r = 0$ Pa) and its initial velocity is also assumed to be zero ($V_r = 0$ m/s). Moreover, the reservoir and the machines are at the same elevation and, therefore, $\Delta Z = Z_M - Z_r = 0$ m. The remaining variables take on values different from zero and the equation (16) is simplified to:

$$h_p = \frac{P_M}{\gamma} + (1 + f\frac{l}{D} + \sum K_{L\ Local})\frac{V^2}{2g} \quad (13)$$

An auxiliary calculation is required to determine f, $\sum K_{L\ Local}$ and V to allow to determine the required pump power.

To use the Colebrook's equation or the Moody's diagram for the first variable (f), one must return to the related rugosity and the Reynolds number presented before in the equations (6) and (7). The flow rate value considered was 120 l/min, meeting the requirements of the machines. The values considered for diameter, roughness, kinematic viscosity, and flow rate matched the characteristics of the pipes and the lubricating oil used and the flow requirements of the machines.

$$\frac{\varepsilon}{D} = 0.0047$$

$$Re = 8020$$

From this follows the Colebrook equation presented in equation (7) get:

$$\frac{1}{\sqrt{f}} = -2\log\left(\frac{\varepsilon/D}{3{,}7065D} + \frac{2{,}5226}{Re\sqrt{f}}\right) => f = 0.0387$$

The same outcome is obtained from the Moody's chart, illustrated in figure 31, albeit more roughly.

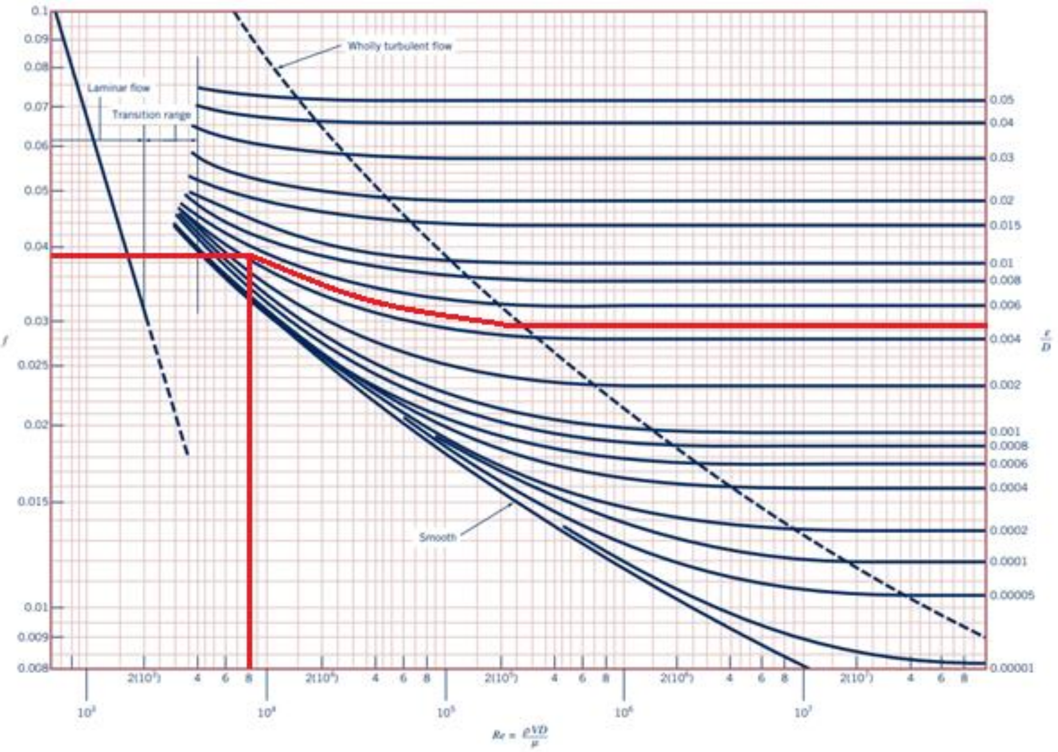

Figure 31 - Friction factor obtained from Moody's diagram.

The calculation of the sum of the local pressure drop coefficients below is based on the table in Annex A and according to the characteristics of the piping associated with the most unfavorable route present in the installations, as follows:

$$\sum K_{L\ Local} = 5 \times Long\ radius\ 90°, threaded + 2 \times Regular\ 45°, threaded + 5 \times Union, threaded + Entrance\ flow + Exit\ flow$$

Thus,

$$\sum K_{L\ Local} = 10.2$$

The last auxiliary calculation (V) is related to determining the oil velocity from the established flow rate given by equation (17):

$$V = V_M = \frac{Q}{A} \tag{14}$$

Thus,

$$V = 2.53 \text{ m/s}$$

Thus, the final equation is obtained considering the pressure desired by the machines and the machine that is furthest from the reservoir, that is, the worst-case scenario. Thus, simplifying the equation (16), obtain:

$$h_p = 93.50 \text{ meters of oil column}$$

Where,

$P_M = 6 \text{ bar} = 600\ 000 \text{ Pa}.$

$\gamma = \rho \times g$

$\rho = 0{,}85 \text{ g/cm}^3 = 850 \text{ kg/m}^3.$

$g = 9{,}81 \text{ m/s}^2.$

$l = 45 \text{ m}.$

These are the column meters of oil that the pump must overcome in order to reach the machines at the desired pressure, allowing for optimal machine operation. This value can be converted to Pa or Bar by the following formula (18):

$$P = h_p \times g \times \rho \tag{15}$$

Thus,

$$P = 779.7 \text{ kPa} \approx 7.80 \text{ bar}$$

This means that the oil distribution system in the facility needs to pump oil with a pressure of approximately 7.8 bar for it to reach the inlet of the working machines with the desired pressure of 6 bar. This allows us to understand that we are facing an installation that is constantly subject to a pressure drop in the order of 1.8 bar for each path drawn between pump and machine. This situation concerns one pump delivering oil to one machine. There are 13 machines in the installation and each one is exclusively associated with a single pump, except for one special case in which a pump is sending oil to 5 different machines.

In order to support this idea, real experimental test was performed to verify the actual head loss to which the distribution system is subjected. Thus, a manometer was placed at the pump outlet and another at the machine inlet and the values were recorded as shown in figures 32 and 33.

Figure 32- Gauge pressure at pump outlet.

Figure 33- Pressure gauge at the machine inlet.

As can be seen, there are pressure losses due to the route taken because the pressure starts out at around 10 bar and drops to about 7 bar near the end. This realistic scenario provides evidence to support the predicted theoretical numbers and illustrates how pressure drops impact the final pressure value. The pressure value declined by around 30% in this particular instance.

The next step to be determined is the available NPSH, present in the following equation (19), fundamental to verify the cavitation situation when compared to the required NPSH, is given by:

$$NPSH_{available} = \frac{Patm\ local}{\gamma} - Z_{suction} - \frac{Pv}{\gamma} - H_{L\ suction} \qquad (16)$$

Each of the terms was determined on an individual basis. The first term was taken from table 19 in annex C and assumed a height value of zero meters above sea level. The second term is related to the distance between the oil suction zone and the pump. The value considered is an average among existing pumps. In annex E is an example of the technical drawing of a pump where the suction height can be seen. In the third term, an estimate of the saturation point value was recorded because the table in annex C, which is linked to the saturation point of water rather than oil, was taken into consideration. In the fourth term, the losses in the short section described in term 2 were calculated. The following are each of the terms listed calculated resulting in:

$$NPSH_{available} = 5.51 \text{ m}$$

Where:

$$\frac{Patm\ local}{\gamma} = 10.33\ m$$

$$Z_{suction} = 0.8\ m$$

$$\frac{Pv}{\gamma} = \frac{33639}{9777} = 3.44\ m$$

$$H_{L\ suction} = 0.36\ m$$

This value of $NPSH_{available}$ mustn't be exceeded in any way by $NPSH_{required}$. This $NPSH_{available}$ value is considered the same for all pumps installed in the plant since they are all under the same conditions for setting this parameter. Regarding $NPSH_{required}$, this will be checked individually while the performance of each pump is analyzed.

Once the NPSH is determined, the conditions are met to check the performance level of each pump. The pumps must meet these requirements to maintain optimum machine operation, otherwise oil supply anomalies may arise. The terms obtained above are summarized as follows:

$$h_p = 93.50 \text{ m or } P = 7.80 \text{ bar}$$

And,

$$Q = 120 \text{ l/min}$$

And,

$$NPSH_{available} = 5.51 \text{ m.c.o.}$$

All pumps are analyzed using the characteristic curves of each pump. On the website of the Danish pump supplier, *Grundfos*, simulations were run with the key parameters as input variables, but also considered the fact that oil was used as the fluid rather than water and that viscosity, density, and the typical operating temperature were all taken into consideration. Figure 34 illustrates a *Grundfos* pump which is installed at the facility. These graphs are available in the appendix F.

Figure 34- Example of a Grundfos pump used in the factory.

The first pump, called *Grundfos* MTRE 15-14/14, is the only one that feeds more than one machine simultaneously. In this case it feeds five machines. The other pumps are all exclusive to just one machine. This pump must be able to deliver more than 120 liters per minute because it will be used to supply oil to multiple machines at once. Specifically, it needs to be able to deliver 600 liters per minute when all five machines are operating at full capacity. However, since this is a unique circumstance, it is extremely unlikely that it would occur in a real-world situation. In fact, in annex F shows that, when the pump curve and the system curve are intersected, the flow rate that the pump can inject at is only around 300 l/min with a total efficiency of 51,4%, i.e., it doesn’t meet the defined requirements.

Moving on to the second pump, the *Grundfos* MTRE 10-12/12, and examine its corresponding graph in Annex F, we can see that it is within the predetermined parameters, indicating that this pump is appropriately sized in terms of flow and head and displaying an efficiency of 49,3%.

Regarding the third pump, the *Grundfos* SPK8-9/9, which is depicted in annex F, even though it can deliver the necessary flow, the head that is currently available is grossly inadequate. This indicates that the fluid enters the machine at a pressure that is significantly lower than ideal. However, if the head value is very low, there is a chance that the pump won't even be able to deliver the oil to the machine, which could result in a very serious lubrication problem. Then, based on equation (16) and removing the pressure portion, the minimum value that the pumps must surpass at least to overcome the pressure losses in the pipelines along the way is given by:

$$h_p = \frac{V_M^2}{2g} + f\frac{l}{D}\frac{V^2}{2g} + \sum K_{L\ Local}\frac{V^2}{2g} \tag{17}$$

Thus, using the same values as before in (16):

$$h_p = 21.5 \text{ m or } P = 1.80 \text{ bar}$$

The calculated value, which was 21.5 m.c.o., was less than the pump's simulation, which was 31 m.c.o. This indicates that the pump is able to fulfill this minimal requirement and prevent serious issues by at least sending the oil to the machine, albeit at a lower pressure than it should.

The next pump, a *Grundfos* CRK4-160/16, is present in the company three times, which means that each of the three pumps in this model feeds a different machine. Once more, appendix F displays the characteristic curve for this pump. Due to the flow rate and pressure being outside of the specified ranges, this pump model also falls short of ideal standards. Since the pump model in question was assembled with three identical units, none of them achieved the desired results. However, this situation isn’t as dramatic as the previous one because these pumps have a much higher height value and don’t compromise the minimum operation.

The following two pumps, *Grundfos* MTR 8-18/15 and *Grundfos* CRK8-200/20, whose graphs can be seen in appendix F, meet the ideal conditions set with a yield of 43.1% and 46.0% respectively.

The final pump, a *Grundfos* MTRE 5-20/20, which is depicted in annex F, has a slight deficit in terms of flow and pressure capacity. Whereas it doesn’t in any way affect the system's minimal operation, it falls short of the objectives set for flawless operation.

Therefore, all pumps were examined with mainly two scenarios being visible: There are pumps that can operate to the expected quality in every way. However, many pumps fall short of maximizing the quality of tool production. Positively, none of the nine pumps under investigation missed the mark of the minimal requirements for overcoming pressure losses along the pipe run. This means that while they might not arrive at the working machines with the desired pressure, they achieve this without incident at their destination. Otherwise, if a tool isn't lubricated during manufacturing, this would be a serious situation that would require immediate intervention, making it impossible to complete the task. The lack of cooling during tool production results in metal expansion, which causes the tool to lag of the specified millimeter dimensions. Due to this problem, the tool would later be rejected by the customer for failing to meet the requirements, which would result in a drop in sales revenue. This demonstrates how crucial this issue is throughout the remainder of the process, up until the customer's final order.

The analysis of all the pumps is summarized in the table 4 that follows. This table was created according to the distribution of the pumps around each of the reservoirs.

Table 4- Summary of the capacity of the pumps installed in the facility.

Reservoir	**Machine**	**Pump**	**Flow Rate [L/min]**	**Pressure [bar]**	**OK/NOK**
UF-0005	PF-14, 23, 31, 42 RT-34	MTRE 15-14/14	360 (600)	7.8	NOK
UF-0005	RT-61	MTRE 10-12/12	120	7.8	OK
UF-0005	PF-37	SPK8-9/9	111	3.2 (7.8)	NOK
UF-0005	RT-36	CRK4-160/16	102 (120)	6.6 (7.8)	NOK
UF-0009	PF-32	CRK4-160/16	102 (120)	6.6 (7.8)	NOK
UF-0009	PF-21	CRK4-160/16	102 (120)	6.6 (7.8)	NOK
UF-0009	PF-34	MTR 8-18/15	132.9	9.4	OK
UF-0009	PF-22	CRK8-200/20	158	13.3	OK
UF-0009	PF-19	MTRE 5-20/20	110 (120)	6.4 (7.8)	NOK

This table lists each pump's associated tank as well as the machine it is meant to operate. The coded tank and machine identities are only destined for internal use to optimize operator communication. The table is introduced in the same order as the analysis above. In addition, when the pump doesn't meet the predetermined values, it shows up in red in the flow and pressure column. The last column defines whether the pump is fully prepared to operate under optimal conditions.

Table 5 shows an estimate of the annual cost of the pumps installed before the intervention. Naturally these values will be a way of comparison with the values that will be estimated after the improvement proposals. These values are obtained from the *Grundfos* supplier's website and aren't real values, just an estimate. This happens because unfortunately there isn't electric meter for the energy consumed exclusively by the pumps, only the general meter for the entire plant. The aim is to analyze the variation that is obtained between these values and those obtained at the end of the changes since they will be subject to the same criteria. In these calculations an energy value per kWh of 8 cents was assumed after checking the electricity statement of the factory. In addition, it was considered that the plant works around 230 days per year with a daily work rate by the pumps of 50%. This means that the pumps work about 2424 hours per year. As can be seen, a cost estimate is being made for non-optimal working conditions, that is, for pumps that don't meet the requirements.

Table 5- Estimated annual cost of each pump before improvement proposals.

Machine	Pump	Target flow rate [l/min]	Calculated flow rate [l/min]	Annual Energy Consumption [€]
PF-14, 23, 31, 42 RT-34	MTRE 15-14/14	600	360	388.40
RT-61	MTRE 10-12/12	120	120	196.75
PF-37	SPK8-9/9	120	111	164.89
RT-36	CRK4-160/16	120	102	190.43
PF-32	CRK4-160/16	120	102	190.43
PF-21	CRK4-160/16	120	102	190.43
PF-34	MTR 8-18/15	120	120	192.40
PF-22	CRK8-200/20	120	120	205.68
PF-19	MTRE 5-20/20	120	110	175.51
			Total:	**1894.92**

After performing the analyses of the pumps that send fluid from the reservoir to the operating machinery, it is now essential to examine the pumps that send fluid in the opposite direction, that is, from the machinery to the reservoir.

Figure 35 shows that when oil is discharged from the machine, it first enters a small tank before being pumped back to the reservoir.

Figure 35- Small tank and pump to return the oil to the reservoir.

When this kind of pump is used, the presence of these tiny tanks is required. This is due to the fact that this particular model of pumps must necessarily be submerged in oil, meaning that the oil level inside the tank is always higher than the level at which the pump. Employing level sensors positioned inside the tank to define when the pump should be turned on or off fulfills this requirement. For instance, to prevent the tank from overflowing, the pump is activated when the oil level in the tank reaches a certain level. Later, it is turned off when the oil level is low in in order to prevent it from dropping to the pump level.

Then, in such a way as to be able to pump the oil back to the reservoir, an analysis was carried out to establish the minimum power that must be implemented to the pumps. The equations are equivalent to those previously employed. In contrast to the initial scenario, where the oil was supposed to reach the reservoir with a pressure of 6 bar, there is no minimum required pressure in this case, so it was assumed to be zero. The remaining attributes stayed unchanged as follows:

$$\frac{P_r}{\gamma} + \frac{V_r^2}{2g} + Z_r + h_p = \frac{P_M}{\gamma} + \frac{V_M^2}{2g} + Z_M + f\,\frac{l}{D}\frac{V^2}{2g} + \sum K_{L\ Local}\frac{V^2}{2g} \tag{18}$$

Simplifying,

$$h_p = (1 + f\,\frac{l}{D} + \sum K_L)\frac{V^2}{2g} \tag{19}$$

Then,

$$h_p = 21.5 \text{ m.c.o. or } P = 1.80 \text{ bar}$$

The installed oil return pumps must meet a minimum requirement of 21.5 m.c.o. or 1.80 bar. Afterwards, these pumps are evaluated to verify the performance criteria. In contrast to the oil release pumps for the machines, these return pumps for the reservoir are all the same model except for one that will be checked later. A catalog from the American company, Xylem, for this specific pump was used to compile the characteristics of the pumps that were installed in the factory, as shown in appendix 6 (Xylem 2022):

The plant currently has pumps of model CO 350/07/D, which are highlighted in appendix 6, and according to the calculations made previously, these pumps fall short of the specifications established for the flow rate of 120 liters per minute. Unfortunately, this means that in order to solve the problem, intervention must be made with all these pumps.

Relative to the only return pump that is of another model, this pump doesn't demand a tank at the machine outlet to store oil above the pump level. This pump is installed as follows in figure 36:

Figure 36- Return pump without auxiliary tank.

As can be seen, this pump's installation is simpler than the others. This is aided by the pump's features, which enable it to send oil only when requested. These features include automatic activation and deactivation. There is no longer a constant concern about having to keep this pump submerged in oil.

The figure present in appendix F details the features of the current pumps produced by Schmalenberger, a German company (Schmalenberger 2022).

The SM 50-13/2 pump, which is present in the factory, is demonstrated in the graph by the area that is highlighted in green. The variables of head and flow rate are used to define the pump once again in this graph, just like they were in the previous ones. The graph shows that this pump can deliver high flow rates without any issues, but the ideal working area for satisfying the established head can only be found in a tiny portion of the graph. Since the pump should function in these circumstances in order to fulfill the requirements, this is not really considered to be a problem.

The analysis of all the return pumps is summarized in the table 6 that follows:

Table 6- Summary of the capacity of the return pumps installed in the facility.

Machine	Return Pump	Flow Rate [l/min]	Pressure [bar]	OK/NOK
PF-14, 19, 21, 22, 23, 31, 32, 34, 42 RT-34, 36, 61	Lowara CO 350/07/D	120	0.9 (1.8)	NOK
PF-37	Schmalenberger GmBH SM 50-13/2	200	1.9	OK

Just like the situation with the oil sending pumps, this table lists each pump's associated machine it is meant to operate. The machine identities are only destined for internal use to optimize operator communication. The table is introduced in the same order as the analysis above. In addition, when the pump doesn't meet the predetermined values, it shows up in red in the flow and pressure column. The last column defines whether the pump is fully prepared to operate under optimal conditions. In conclusion, under the given circumstances, only one return pump is fully functional. The available head presents a challenge to all the others.

Checking the reservoirs' capacity, or whether their size is appropriate for the number of machines they are connected to, is another pertinent factor. Consequently, the reservoirs' size was estimated considering that distinct calculations were performed for each tank. The objective is that the amount of oil that reaches the contaminated part of the tank per minute is less than the amount that is filtered, cooled, and passes into the clean oil compartment ready to be released again. At first, the distance that the oil traveled between the reservoir and the machine was calculated as follows:

$$L_{Total} = L_{Tubo} + L_{Equiv} \quad (20)$$

L_{Equiv} can be calculated by equation (23):

$$L_{Equiv} = \frac{\sum K_L \times D}{f} = 8.37\text{m} \quad (21)$$

Therefore, being $L_{Tube} = 45$ m then,

$$L_{Total} = 53.37 \text{ m}$$

In fact, by converting to equivalent length, this value of L_{Equiv} equals all local pressure losses along the entire path associated with existing bends and fittings.

The time taken by each component to complete the entire oil journey is given by equation (25) and (26):

$$Time_{Path} = Time_{Return\ Path} = \frac{L_{Total}}{V} \tag{22}$$

$$Time_{Filtration\ 1} = Time_{Filtration\ 2} = \frac{Q \times NM \times 60}{FC} \tag{23}$$

Where,

$V = Velocity\ of\ oil$ (m/s)

$Q = Oil\ Flow\ Rate$ (l/min)

$NM = Number\ of\ machines\ associated\ with\ the\ reservoir$

$FC = Filtration\ Capacity$ (l/min)

Solving these equations:

$$Time_{Path} = Time_{Return\ Path} \approx 21 \text{ s}$$

And,

$$Time_{Filtration\ 1} = 126 \text{ s}$$

And,

$$Time_{Filtration\ 2} = 108 \text{ s}$$

Therefore, the total time spent is given by equation (27):

$$Time_{Total} = Time_{Path} + Time_{Filtration} + Time_{Return\ Path} \tag{24}$$

Then,

$$Time_{Total\ 1} = 168 \text{ s} \approx 2.80 \text{ min}$$

And,

$$Time_{Total\ 2} = 150 \text{ s} \approx 2.50 \text{ min}$$

The duration of time required to complete a full circuit for each tank is 2.5 minutes for one tank and 2.8 minutes for the other. Because it only lasts for a very short amount of time, the time the oil is present in the machine was neglected in these calculations.

Next, the number of liters each machine needs for each tank was determined using equation (28).

$$l/machine = Time_{Total\ 1} \times Q \tag{25}$$

Thus,

$$Time_{Total\ 1} \times Q = 336 \text{ l/machine}$$

And,

$$Time_{Total\ 2} \times Q = 300 \text{ l/machine}$$

It should be noted that the reason for the differences in the values for each tank is that one tank feeds one more machine than the other, which outcomes in a slight delay in the filtration process.

Finally, the required capacity can be determined and compared with the reservoirs' actual capacity as follows:

$$Capacity_{Theorical\ 1} = Capacity_{Theorical\ 2} = l/machine \times NM \qquad (26)$$

From this obtain:

$$Capacity_{Theorical\ 1} = 2355 \text{ l}$$

And,

$$Capacity_{Theorical\ 2} = 1802 \text{ l}$$

The following table 7, which summarizes the analysis of the two reservoirs and compares the theoretical capacity with the real capacity of the contaminated reservoir compartment:

Table 7- Summary of reservoir storage capacity

Reservoir	Required Capacity [l]	Real Capacity [l]	OK/NOK
UF-0005	2355	2500	OK
UF-0009	1802	1750	NOK

Table 7 shows that, if all machines were operating simultaneously, both reservoirs would be very close to, if not exceeded their capacity for the required capacities. This presents yet again another problem.

By changing the subject and concentrating exclusively on the filtration system, its filtration effectiveness will be evaluated. Each reservoir has a total of 400 l/min of filtration through its four filtration towers, each of which has a capacity of 100 l/min.

The following table 8, which summarizes the analysis regarding the filtration capacity of the reservoirs:

Table 8- Summary of the reservoirs' filtration capacity.

Reservoir	Filtration Required Capacity [l/min]	Filtration Capacity [l/min]	OK/NOK
UF-0005	840	400	NOK
UF-0009	720	400	NOK

The results for the necessary filtration capacity were calculated under the worst-case scenario, in which all the equipment connected to the reservoirs would be running simultaneously. Most likely, this scenario rarely materializes, i.e., the current filtration values might be adequate under typical circumstances.

The chillers are the final diagnostics-related topic to be discussed. These chillers, as previously mentioned, have a flow rate of 63.3 l/min. The power required to cool the oil is given by equation (30):

$$P = Q \times c \times GE \times \Delta T \qquad (27)$$

Where,

$P = Power\ (kW)$

$Q = Flow\ Rate\ (l/s)$

$c = Specific\ Heat\ of\ the\ oil\ \ (kJ/kg.K)$

$GE = Specific\ Gravity\ (kg/l)$

$\Delta T = Oil\ Temperature\ Variation\ (T)$

A value of 1.970 KJ/kg. K for the oil's specific value and a specific gravity of 0.88 kg/l were taken into consideration in order to determine the power necessary to cool the oil. The worst-case scenario for the temperature variation was assumed to be 6°C, which means that the oil would reach a temperature of 32°C. The ideal oil temperature is set at 26°C. This results in the following:

$$P = 10.97\ kW$$

This calculation applies to both chillers due to their equivalent power values. These values are within the chillers' established power limitations. Thus, the chillers are adequately sized and equipped to withstand the hot days.

4.2. Improvement proposals

Given the issues identified in the diagnosis carried out in the preceding section, it is essential to look for solutions to the challenges encountered and, thereby, lead to an overall stability of the entire oil distribution system.

The first proposed improvement to the facility is associated with the replacement of the piping. As a result of being in use for more than 20 years, the pipeline in its current state is already worn out and has accumulated residues inside of it that impair oil from passing through it. Although this loss factor has not been quantified, it has the potential to aggravate the load losses in real context. Therefore, it was suggested to install a new pipe with a different material and diameter, which was expected to enhance the system's performance. In contrast to the previous pipe, which had a diameter of 31.75 mm, this one would have a diameter of 38.10 mm and be made of stainless steel rather than galvanized iron. This change in pipeline dimensions translates into an equivalent change in diameter from 1.25 inches to 1.50 inches, a size often used in pipes. The new material is 10 times less rough than the old one, with only a 0.015 mm roughness. This suggestion was taken into consideration and the new piping was implemented as shown in the following figure 37:

Figure 37- New stainless-steel piping.

The calculations noted below are intended to validate the provided proposal. Retrieving equation (16) again given by:

$$h_p = \frac{P_M}{\gamma} + (1 + f\frac{l}{D} + \sum K_{L\ Local})\frac{V^2}{2g}$$

Additionally, by modifying the Reynolds number and relative roughness value for this new material results in values of $Re = 6684$ and $\varepsilon/D = 0.000394$, from which Colebrook's equation yields a new Darcy factor value. This new value obtained is: $f = 0.0349$. The local pressure drop values are unaffected by the piping change, so the sum of the coefficients remains at 10.2. The velocity of the oil in the pipe, as a consequence of the change in diameter, is the last value in the equation that needs to be adjusted. The velocity obtained by applying equation

10 to the new diameter is 1.75. From here, the previous equation can be calculated giving the following outcome:

$$h_p = 80.18 \text{ m}$$

This is the new value that the pump should achieve in order to reach the machines at the desired pressure, allowing for optimal machine operation. Once more using equation 10, this amount can be transformed into:

$$P = 668.6 \text{ kPa} \approx 6.69 \text{ bar}$$

This means that the facility's oil distribution system must pump oil at a pressure of nearly 6,69 bar for it to arrive at the working machines' inlets with the desired pressure of 6 bar.

The values obtained using the proposed pipe and the old pipe are presented in the table 9.

Table 9- Comparison between existing and proposed piping

	Current Situation	**Proposed Situation**
Pipe Diameter [mm]	31.75	38.10
Roughness [mm]	0.15	0.015
Required Operating Head [m.c.o.]	93.50	80.18
Required pressure [Bar]	7.80	6.69

The proposed piping requires a much lower pressure value than the pipeline that is currently in use. The following equation (31) allows to calculate the percentage of pressure reduction:

$$P_{Red} = \frac{(P_{RO} - P_M) - (P_{RP} - P_M)}{(P_{RO} - P_M)} \quad (28)$$

Where,

P_{Red} = Pressure Reduction Percentage.

P_{RO} = Required Pressure using the old tubing.

P_{RP} = Required Pressure using the proposed piping.

P_M = Required Pressure Required at the machine inlet.

Solving the equation (31) obtain:

$$P_{Red} = 61.7\%$$

In fact, the system obtains a pressure reduction from 7.80 bar to 6.69 bar through to operate at its peak, which resulted in a 61.7% decrease in the head losses linked with the circuit. This reduction already makes a significant difference because it relieves the strain on the pumps by reducing the requirements imposed on them. However, this change does not entirely fix any of the concerns which were visible.

The next step in the improvement process would be to fix the problem with the incapacitated pumps. Thus, the solution proposed is to switch out the current pumps for new ones. In accordance with their circumstances, these new pumps would be able to feed multiple pumps at once. The idea of clustering pumps from the same reservoir was taken into consideration. Once again, the *Grundfos* supplier website was used to search for suitable pumps. Retrieving Table 4 with the “NOK” pumps, the following pump groups were formed accompanied by the suggested replacement pump and the machines it will supply. Table 4's situations are all divided into three groups, that can be seen below.

In the first situation, Table 10 lists the CRK4-160/16 pump and the MTRE 15-14/14 pump that are connected to 6 machines. It is intended to limit the MTRE 15-14/14 pump's load to three machines because it can’t deliver oil to five machines at once while the other pump must be replaced by a new one.

Table 10- Pump problem nº1

Machine	Pump	Flow Rate [l/min]	Pressure [bar]	OK/NOK
PF-14, 23, 31, 42; RT-34	MTRE 15-14/14	360 (600)	6.7	NOK
RT-36	CRK4-160/16	102 (120)	6.6 (6.7)	NOK

The two machines that don’t continue to be connected to the previous pump join the RT-36 machine. The following pump, MTRE 20-10/10, is obtained as a solution for this situation after research and simulation of the on-site pumps with the characteristics to support the work of three machines simultaneously. The characteristic curve of this pump can be seen in the appendix F. Table 11 shows the solution for this first pump cluster.

Table 11- Solution for Pump problem nº1

Machine	Pump	Flow Rate [l/min]	Pressure [bar]	OK/NOK
PF-14, 23, 31	MTRE 15-14/14	360	6.7	OK
PF-42; RT-34, 36	MTRE 20-10/10	360	6.7	OK

The distribution of oil from the pump to the different routes is done through a manifold as illustrated in figure 38.

Figure 38- Manifold distributing oil through three different paths.

Regarding the second scenario, there is only one pump present because it is the only one left to solve from this reservoir, as shown in table 12.

Table 12- Pump Problem n°2

Machine	Pump	Flow Rate [l/min]	Pressure [bar]	OK/NOK
PF-37	MTRE 10-9/9	111	3.2 (6.7)	NOK

This device cannot at all meet the requirements, so an alternative pump known as SPK 8-9/9 was discovered using the supplier's website, as illustrated in Table 13.

Table 13- Solution for Pump problem n°2

Machine	Pump	Flow Rate [l/min]	Pressure [bar]	OK/NOK
PF-37	SPK8-9/9	120	6.7	OK

The final problem concerns the three pumps that were installed on the second reservoir but just do not meet the specifications. In table 14, these pumps are displayed.

Table 14- Pump Problem nº3

Machine	Pump	Flow Rate [l/min]	Pressure [bar]	OK/NOK
PF-32	CRK4-160/16	102 (120)	6.6 (7.8)	NOK
PF-21	CRK4-160/16	102 (120)	6.6 (7.8)	NOK
PF-19	MTRE 5-20/20	110 (120)	6.4 (7.8)	NOK

As in previous cases, an attempt was made to replace these three pumps with a single one that would work for all 3 machines. Thus, the MTRE 20-10/10 pump is selected as the pump proposal found, which is the same as in case number 1. Table 15 displays the three machines connected to the proposed new pump.

Table 15- Solution for Pump problem nº3

Machine	Pump	Flow Rate [l/min]	Pressure [bar]	OK/NOK
PF-32, 21, 19	MTRE 20-10/10	360	6.7	OK

If we redo the table of annual energy costs (table 5) with these changes, we realize that there is a decrease in the number of pumps in the plant. This is due to the association of the new pumps to more than one machine at the same time. In this way, the space occupied by these pumps in the factory is reduced. The summary of the energy costs is shown in table 16.

On the other hand, and fulfilling the main objective, the dimensioned pumps meet the established requirements, promoting a good operation of the oil distribution system.

Finally, we also highlight the fact that it was possible to reduce the energy consumption associated with the pumps, that is, there was an optimization in the process.

Table 16 - Estimated annual cost of each pump after improvement proposals.

Machine	Pump	Target flow rate [l/min]	Calculated flow rate [l/min]	Annual Energy Consumption [€]
PF-14, 23, 31	MTRE 15-14/14	360	360	388.40
PF-42, RT-34, 36	MTRE 20-10/10	360	360	332.57
RT-61	MTRE 10-12/12	120	120	196.75
PF-37	MTRE 10-9/9	120	120	162.22
PF-32, 19, 21	MTRE 20-10/10	360	360	332.57
PF-34	MTR 8-18/15	120	120	192.40
PF-22	CRK8-200/20	120	120	205.68
			Total:	**1810.59** **-4.7%**

Once the improvement proposals for the pumps feeding the machines are finalized and all the problems associated with this issue have been addressed, it is time to address the problem found in the previous section regarding the pumps pumping from the machines to the reservoir. Referring to table 6, almost every pump has trouble when oil is pumped back into the reservoir. In this analysis, galvanized iron pipes were used. Because the pressure drop value is much lower using the suggested piping, these pumps are once again examined. Therefore, equation 10 is used once again and replace the variables with the values associated with this new stainless-steel pip, resulting in:

$$h_p = 8.22 \text{ m or } P = 0.69 \text{ bar}$$

The result is the new value that the pump must surpass in order to operate under what is assumed to be the right circumstances. Surprisingly, it can be seen from Table 15, which lists the pump's technical specifications, that by doing so, the pump is already capable of compensating for the head losses that are currently present, making this pump model appropriate for use with the new piping conditions.

According to table 17, these pumps don't require any modifications or replacement because all that is required to enable efficient oil pumping is to change the piping.

Table 17- Solution for return pumps.

Machine	Return Pump	Flow Rate [l/min]	Pressure [bar]	OK/NOK
PF-14, 19, 21, 22, 23, 31, 32, 34, 42 RT-34, 36, 61	Lowara CO 350/07/D	120	0.9	OK

However, if there are plans to invest in new equipment and optimize the factory, there is an additional problem that can be resolved. The return pumps used, except one, are attached to a small tank before sending the oil back to the reservoir. The idea is to get rid of the tank and use only return pumps. To make this happen, all these pumps would have to be replaced with a model that is the same as the exclusive pump in the plant. This unique pump is well sized. The only drawback to these changes is related to the investment that would have to be made to acquire so many pumps.

5. Conclusions and future work

This dissertation was based on the evaluation of the equipment's operational conditions related to the oil lubrication system in Grinding machines. The optimal functioning of this lubrication system depends fundamentally on 3 aspects: the oil distribution system, the filtration system, and the cooling system. It was possible to understand throughout the project that these 3 factors are interconnected and that the existence of problems in one of them influence the functioning of the others, affecting the whole lubrication system. In this way, each of them was analyzed individually.

The oil distribution system was the topic that received the most attention because, upon diagnosis, it presented the biggest potential failures. The fluid seems to have a greater difficulty passing through old piping because it has more friction. It was possible to observe, through an experimental test, the significant impact that pressure losses have on circuit development. These result in a pressure value reduction of about one-third of the initial pressure. This is also because these pipelines are made of a material that is outdated especially in comparison to the materials used today, which have better properties. Additionally, the factory production of cutting tools must conform to very specific parameters in order to guarantee high quality. Sometimes this situation didn't occur in a good part of the pumps that launched the oil to the machines because the pumps lacked the capacity to deliver the oil to the machines at the proper pressure and flow rate.

Regarding these problems, the initial solution proposal was to change the pipes' composition from galvanized iron to stainless steel because the roughness is 10 times lower. In addition, the pipe diameter was increased by 20%, which had a more considerable impact on the system. In fact, putting these 2 specifications into practice enables a 62% reduction in the associated head losses. Concerning the situation of the pumps, the improvement solution involved replacing the current pumps with new, more powerful ones which in certain cases could feed up to 3 machines at the same time. The use of the new piping simplifies this task considerably. In this way, there are a reduction of pumps that are running simultaneously. From the simulations performed, it was possible to obtain a 4.7% reduction in the energy used to power the pumps and at the same time meet the requirements established in the project.

The final suggestion on this topic of oil distribution system is based on the pumps that transport used oil from the machines back to the reservoir. The pumps with this task were almost all the same model and presented problems in sending oil. Fortunately, the solution related to changing the piping mentioned above fixes this problem.

As for the filtration system, the currently operational installation is capable of handling most everyday situations. Only in very extreme situations is it incompatible, and the solution would be to purchase and connect a new filtration tower. However, this measure would be unaffordable due to the associated costs and the return that this would bring.

The last situation refers to the cooling system, which is like the filtration system. The current system is viable for most days of the year, only falling short in very extreme heat situations. In these cases, the ambient temperature of the plant, the heat generated by the machines and pumps make it very difficult to correctly cool the oil. Obviously, an effective solution would be the support with one more chiller, but the investment would not bring enough benefits for the annual energy expenses.

In this context of the oil lubrication system, it would be interesting to go a little deeper into some topics that unfortunately have not been fully covered such as the following:

- Acquisition of a flow meter to verify what the real oil consumption is in each machine. Throughout this project the flow rate established by the machines' manual was always adopted due to this lack of material. This assumption was one of the bases for the simulations performed on the pumps.
- Further analysis related to heat transfers between the elements involved. The idea would be to quantify in more detail the heat released by the pumps into the oil when they are pumping it and the heat generated in the oil when the tool is being produced, although in some articles there are already some estimates. Finally, analyze the relevance of fitting insulation around the existing piping throughout the factory to protect from heat and cold since the oil must always remain at controlled temperatures.
- The placement of an energy meter in some strategic points such as at the pumps or machines to understand the real consumption they have over time. Currently only the general counter of the factory is available, which accounts for all the electrical devices present in the factory.
- Performing an analysis on the possible occurrence of water hammer in the pipes. This phenomenon is caused by the sudden change of pressure in the pipes when valves or flow is interrupted.
- Analyze a possible implementation of a software that allows remote monitoring of the status of machines, pumps, chillers and filtration towers in order to act, promptly, to some adverse situation and obtain a history of the performance of each device.

References

Bilgen, S. 2014. *Structure and environmental impact of global energy consumption.* Renewable and Sustainable Energy Reviews. doi:http://dx.doi.org/10.1016/j.rser.2014.07.004.

Broomer, S. Y. Hong & M. 2000. *Economical and ecological cryogenic machining of AISI 304 austenitic stainless steel.* Clean Products and Processes. doi:https://doi.org/10.1007/s100980000073.

Carlos Rogério de Mello, Tadayuki Yanagi jr. 2010. "Escolha de Bombas Centrífugas."

Edson Ezequiel de Mattos, Reinaldo de Falco. 1998. *Bombas Industriais.* Interciência.

FUCHS SCHMIERSTOFFE GMBH. 2017. "Cutting Fluids – Monitoring and Maintenance." 20.

Grundfos. 2022. *Size your pump.* https://product-selection.grundfos.com/pt.

H.K. Tönshoff, B. Karpuschewski, T. Mandrysch, I. Inasaki,. 1998. *Grinding Process Achievements and their Consequences on Machine Tools Challenges and Opportunities.* CIRP Annals, 651-668. doi:https://doi.org/10.1016/S0007-8506(07)63247-8.

HardHat Engineer. 2022. *Centrifugal Pump Diagram.* https://hardhatengineer.com/centrifugal-pump-diagram/.

HVAC Investigators. 2022. *The Basics of Chillers.* Alpine Intel. Dezembro 2. https://www.hvacinvestigators.com/webinars/the-basics-of-chillers-how-they-work-where-theyre-used-and-common-problems/.

José Martiniano de Azevedo Netto, Miguel Fernández y Fernández. 2015. *Manual de Hidráulica.* Blucher.

Lin, Kuan-Ming Li & Cheng-Peng. 2011. *Study on minimum quantity lubrication in micro-grinding.* The International Journal of Advanced Manufacturing Technology. doi:10.1007/s00170-011-3789-1.

M. Bhuyan, A. Sarmah, K.K. Gajrani, A. Pandey, T.G. Thulkar, M.R. Sankar. 2018. *State of Art on Minimum Quantity Lubrication in Grinding Process.* Materials Today: Proceedings, 19638-19647. doi:https://doi.org/10.1016/j.matpr.2018.06.326.

M., Haynes W. 2014. *Handbook of chemistry and physics 95th edition.* CRC Press.

Mohamed Osama, Amarpreet Singh, Rashmi Walvekar, Mohammad Khalid, Thummalapalli Chandra Sekhara Manikyam Gupta, Wong Wai Yin. 2017. *Recent developments and performance review of metal working fluids.* Tribology International. doi:https://doi.org/10.1016/j.triboint.2017.04.050.

Navneet Khanna, Prassan Shah, Murat Sarikaya, Franci Pusavec. 2022. *Energy consumption and ecological analysis of sustainable and conventional cutting fluid strategies in machining 15–5 PHSS.* Sustainable Materials and Technologies. doi:https://doi.org/10.1016/j.susmat.2022.e00416.

Observatório da Energia, DGEG, ADENE. 2022. *Energia em Números.* ADENE – Agência para a Energia.

Pei Yan, Yiming Rong, Gang Wang. 2015. *The effect of cutting fluids applied in metal cutting process.* Proceedings of the Institution of Mechanical Engineers. doi:https://doi.org/10.1177/0954405415590993.

Philip M. Gerhart, Andrew L. Gerhart, John I. Hochstein. 2016. *Munson, Young and Okiishi's fundamentals of fluid mechanics*. John Wiley & Sons.

Precedence Research. 2020. "Industrial Lubricants Market." https://www.precedenceresearch.com/industrial-lubricants-market.

Qingyu MENG, Bing GUO, Qingliang ZHAO, Hao Nan LI, Mark J. JACKSON, Barbara S. LINKE, Xichun LUO. 2022. "Modelling of grinding mechanics: A review." doi:https://doi.org/10.1016/j.cja.2022.10.006.

R. Rekha, S. Vinoth Kumar, V. Aravinth Raj, B. Aswin Baboo, P. Gokul Raj, A. Jai Vignesh. 2022. *Optimization of cylindrical grinding process parameters on austenitic stainless steel 304 using Taguchi based Grey Relational Analysis*. Materials Today: Proceedings. doi:https://doi.org/10.1016/j.matpr.2022.10.120.

Roser, Hannah Ritchie and Max. 2022. *Energy Production and Consumption*. Our World in Data. https://ourworldindata.org/energy.

Saikat Chatterjee, Ramesh Rudrapati, Pradip Kumar pal, Goutam Nandi. 2018. "Experiments, analysis and parametric optimization of cylindrical traverse cut grinding of aluminium bronze." 5272-5280. doi:https://doi.org/10.1016/j.matpr.2017.12.110.

Saroj Kumar Patra, Suchismita Swain. 2022. *Effects of minimum quantity lubrication (MQL) in grinding: Principle, applications and recent advancements*. Materials Today: Proceedings, 96-106. doi:https://doi.org/10.1016/j.matpr.2022.08.157.

Schmalenberger. 2022. *Self-priming centrifugal pumps type SM*. Dezembro 7. https://schmalenberger.de/en/pump/type-sm/.

Şenol Şirin, Murat Sarıkaya, Çağrı Vakkas Yıldırım, Turgay Kıvak. 2021. *Machinability performance of nickel alloy X-750 with SiAlON ceramic cutting tool under dry, MQL and hBN mixed nanofluid-MQL*. Tribology International. doi:https://doi.org/10.1016/j.triboint.2020.106673.

T. Tawakoli, M.J. Hadad, M.H. Sadeghi. 2010. *Investigation on minimum quantity lubricant-MQL grinding of 100Cr6 hardened steel using different abrasive and coolant–lubricant types*. International Journal of Machine Tools & Manufacture, 698-708. doi:https://doi.org/10.1016/j.ijmachtools.2010.04.009.

Tsutiya, Milton Tomoyuki. 2006. *Abastecimento de água*. São Paulo: Departamento de Engenharia Hidráulica e Sanitária da Escola Politécnica da Universidade de São Paulo.

White, Frank M. 2016. *Fluid Mechanics*. McGraw-Hill Education.

Xylem. 2022. *Tabela de Preços*. rolearmais.

Zishan Ding, Jian Sun, Weicheng Guo, Xiaohui Jiang, Chongjun Wu & Steven Y. Liang. 2021. *Thermal Analysis of 3J33 Grinding Under Minimum Quantity*. International Journal of Precision Engineering and Manufacturing-Green Technology. doi:https://doi.org/10.1007/s40684-021-00391-y.

Appendix A: Local Roughness and Head Loss Coefficient

In this appendix, pipe characteristics related to material and roughness are shown in Table A-1. In addition, the coefficients associated with local head losses appear in figure A-1 and A-2 and tables A-2.

Table 18- Roughness Values for commercial Ducts

		ε		
Material	**Condition**	**ft**	**mm**	**Uncertainty, %**
Steel	Sheet metal, new	0.00016	0.05	±60
	Stainless, new	0.000007	0.002	±50
	Commercial, new	0.00015	0.046	±30
	Riveted	0.01	3.0	±70
	Rusted	0.007	2.0	±50
Iron	Cast, new	0.00085	0.26	±50
	Wrought, new	0.00015	0.046	±20
	Galvanized, new	0.0005	0.15	±40
	Asphalted cast	0.0004	0.12	±50
Brass	Drawn, new	0.000007	0.002	±50
Plastic	Drawn tubing	0.000005	0.0015	±60
Glass	—	Smooth	Smooth	
Concrete	Smoothed	0.00013	0.04	±60
	Rough	0.007	2.0	±50
Rubber	Smoothed	0.000033	0.01	±60
Wood	Stave	0.0016	0.5	±40

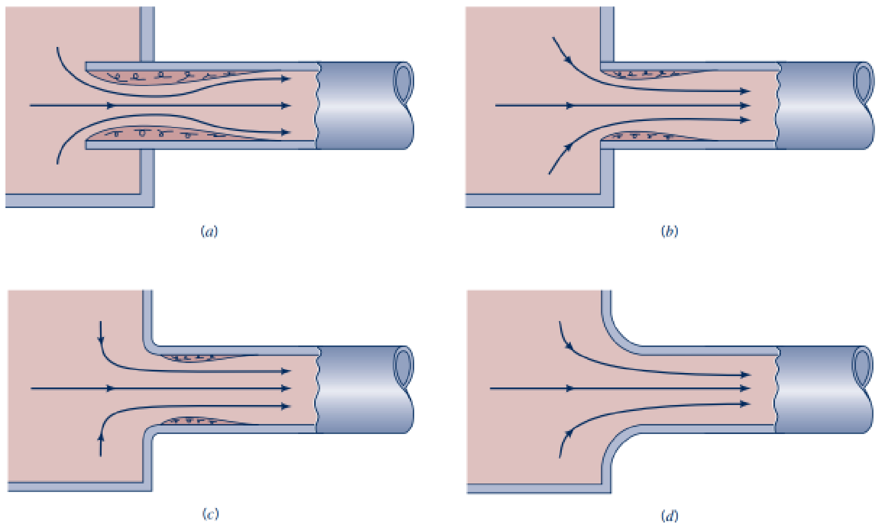

Figure 39- Entrance flow conditions and loss coefficient: (a) Reentrant, K_L = 0.8, (b) sharp-edged, K_L = 0.5, (c) slightly rounded, K_L = 0.2, (d) well-rounded, K_L = 0.04 (Philip M. Gerhart 2016).

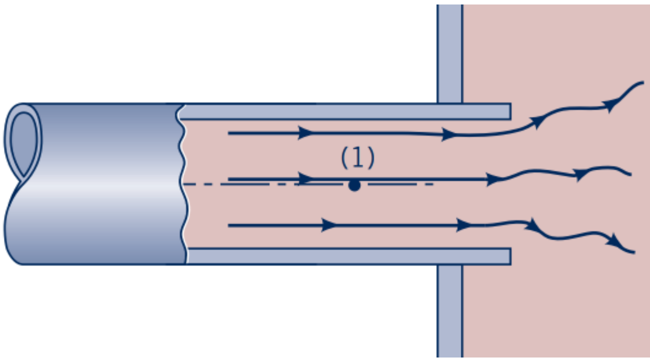

Figure 40- Exit flow loss coefficient, $K_L = 1$ (Philip M. Gerhart 2016).

Table 19- Loss Coefficients for Pipe Components (Philip M. Gerhart 2016)

Component	K_L
a. Elbows	
Regular 90°, flanged	0.3
Regular 90°, threaded	1.5
Long radius 90°, flanged	0.2
Long radius 90°, threaded	0.7
Long radius 45°, flanged	0.2
Regular 45°, threaded	0.4
b. 180° return bends	
180° return bend, flanged	0.2
180° return bend, threaded	1.5
c. Tees	
Line flow, flanged	0.2
Line flow, threaded	0.9
Branch flow, flanged	1.0
Branch flow, threaded	2.0
d. Union, threaded	0.08
***e. Valves**	
Globe, fully open	10
Angle, fully open	2
Gate, fully open	0.15
Gate, $\frac{1}{4}$ closed	0.26
Gate, $\frac{1}{2}$ closed	2.1
Gate, $\frac{3}{4}$ closed	17
Swing check, forward flow	2
Swing check, backward flow	∞
Ball valve, fully open	0.05
Ball valve, $\frac{1}{3}$ closed	5.5
Ball valve, $\frac{2}{3}$ closed	210

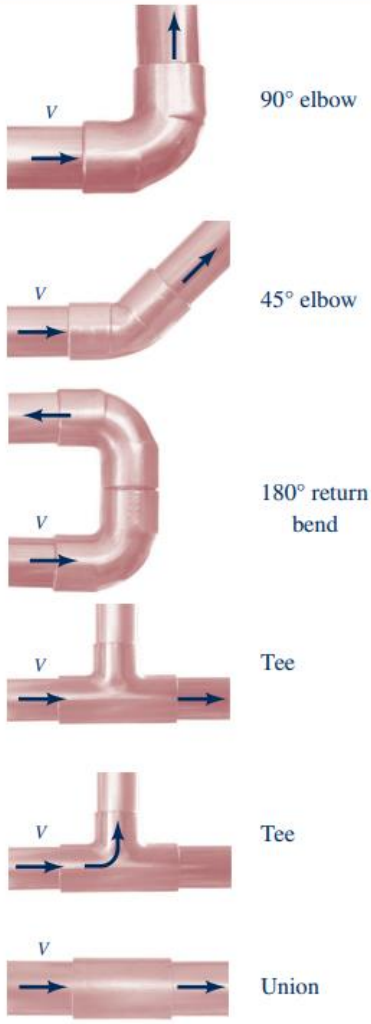

Appendix B: Oil Technical Specifications

The characteristics and properties of the oil the company chose are expressed.

Art.No 3281 - 56

Blasogrind HC 10

Description

High performance grinding oil based on synthetic oil

Range of application

Operations: tool-grinding, tool-regrinding. Other grinding operations after recommendation of our grinding specialists.
Materials: tungsten carbide, high speed steel (HSS) and cermet (under our recommendation it can be also used for other materials).

Product properties		Benefits
Hydrocracked	→	Higher flash point and reduced emissions compared to mineral oils Good machine compatibility
Excellent removing performances	→	Better surface quality Higher grinding wheel life
Low viscosity	→	Good wetting Good rinsing
Cobalt deactivated	→	Specially suitable for grinding of tungsten carbide without cobalt leaching
Colorless	→	Visually clean machines Good process visibility

Physical-chemical data

	Typical data		Measuring method
Viscosity at 40°C	10 mm^2/s		ISO 3104
Density at 20°C	0.85 g/cm^3		DIN 51757
Flash point	180°C		ISO 2592 (COC)
Ester content	3%		
Chlorine content	0%		
Zinc content	0%		
Sulphur content, total	0.8%		
Copper corrosivity	1a	(3h at 60°C)	ISO 2160
Colour	colourless	(ASTM-Colour: 0.5)	

Note

Suitable for edgecap and precoated filter.

Safety and environmental aspects

EC waste code: 12 01 10
ADR-class: none
Water endangering class: WEC 1
For more detailed information please consult the EC Safety Data Sheet.

Information contained in this data sheet is based upon the properties and applications of use as known to us. However, generally no legal liability may be deducted from such information.
0675 01.07.2016 V 06

Appendix C: Values of Atmospheric Pressure and Vapor Pressure

In this section is table C-1 and table C-2 which shows how the atmospheric pressure varies with altitude and the vapor pressure value, respectively.

Table 20- Maximum suction heights

Height[m]	Atmospheric pressure [m.c.o.]
0	10,33
300	10,00
600	9,64
900	9,30
1200	8,96
1500	8,62
1800	8,27
2100	8,00
2400	7,75
2700	7,50
3000	7,24

Table 21- Vapor Pressure and Other Saturation Properties of Water

t °C	P kPa	$\Delta_{vap}H$ kJ kg^{-1}	Surf. Ten. mN m^{-1}	t °C	P kPa	$\Delta_{vap}H$ kJ kg^{-1}	Surf. Ten. mN m^{-1}
0.01	0.61165	2500.9	75.65	80	47.414	2308.0	62.67
2	0.70599	2496.2	75.37	82	51.387	2302.9	62.31
4	0.81355	2491.4	75.08	84	55.635	2297.9	61.94
6	0.93536	2486.7	74.80	86	60.173	2292.8	61.56
8	1.0730	2481.9	74.51	88	65.017	2287.6	61.19
10	1.2282	2477.2	74.22	90	70.182	2282.5	60.82
12	1.4028	2472.5	73.93	92	75.684	2277.3	60.44
14	1.5990	2467.7	73.63	94	81.541	2272.1	60.06
16	1.8188	2463.0	73.34	96	87.771	2266.9	59.68
18	2.0647	2458.3	73.04	98	94.390	2261.7	59.30
20	2.3393	2453.5	72.74	100	101.42	2256.4	58.91
22	2.6453	2448.8	72.43	102	108.87	2251.1	58.53
24	2.9858	2444.0	72.13	104	116.78	2245.8	58.14
25	3.1699	2441.7	71.97	106	125.15	2240.4	57.75
26	3.3639	2439.3	71.82	108	134.01	2235.1	57.36
28	3.7831	2434.6	71.51	110	143.38	2229.6	56.96
30	4.2470	2429.8	71.19	112	153.28	2224.2	56.57
32	4.7596	2425.1	70.88	114	163.74	2218.7	56.17
34	5.3251	2420.3	70.56	116	174.77	2213.2	55.77
36	5.9479	2415.5	70.24	118	186.41	2207.7	55.37
38	6.6328	2410.8	69.92	120	198.67	2202.1	54.97
40	7.3849	2406.0	69.60	122	211.59	2196.5	54.56
42	8.2096	2401.2	69.27	124	225.18	2190.9	54.16
44	9.1124	2396.4	68.94	126	239.47	2185.2	53.75
46	10.099	2391.6	68.61	128	254.50	2179.5	53.34
48	11.177	2386.8	68.28	130	270.28	2173.7	52.93
50	12.352	2381.9	67.94	132	286.85	2167.9	52.52
52	13.631	2377.1	67.61	134	304.23	2162.1	52.11
54	15.022	2372.3	67.27	136	322.45	2156.2	51.69
56	16.533	2367.4	66.93	138	341.54	2150.3	51.27
58	18.171	2362.5	66.58	140	361.54	2144.3	50.86
60	19.946	2357.7	66.24	142	382.47	2138.3	50.44
62	21.867	2352.8	65.89	144	404.37	2132.2	50.01
64	23.943	2347.8	65.54	146	427.26	2126.1	49.59
66	26.183	2342.9	65.19	148	451.18	2119.9	49.17
68	28.599	2338.0	64.84	150	476.16	2113.7	48.74
70	31.201	2333.0	64.48	152	502.25	2107.5	48.31
72	34.000	2328.1	64.12	154	529.46	2101.2	47.89
74	37.009	2323.1	63.76	156	557.84	2094.8	47.46
76	40.239	2318.1	63.40	158	587.42	2088.4	47.02
78	43.703	2313.0	63.04	160	618.23	2082.0	46.59

Appendix D: Chiller Technical Specifications

The catalog with technical data relative to the chillers is present in this attachment.

ENR SERIES

Aircooled liquid chillers ENR series, scroll compressors, plate / coaxial evaporator, condenser with copper tubes, aluminium finned core and axial fans
Luftgekühlte Kältemaschinen ENR Serie, Scroll Kompressoren R410A, Plattenverdampfer / Koaxialverdampfer, Kondensatoren mit Kupfer Leitungen , Lamellenrippen aus Aluminium und Axial-Ventilatoren

Process Cooling Application	*Industriellen Kühlung*		Model	001	002	003	004	005	008	010	012	016	018	022
NOMINAL COOLING CAPACITY (1)	NENNKÄLTELEISTUNG (1)		kW	1,6	2,1	3,6	4,2	5,5	7,9	9,3	12,2	13,5	18	22,0
TOTAL COMPRESSORS NOMINAL ABSORBED POWER (1)	NENNLEISTUNGSAUFNAHME VERDICHTER(1)		kW	0,5	0,7	1,2	1,4	1,8	2,6	3,4	3,9	5,2	5,8	6,7
EER	EER			2,97	2,59	2,79	2,82	2,89	2,77	2,55	2,78	2,37	2,78	2,93
SEPR (HT) (5)	SEPR (HT) (5)			4,7	4,6	4,7	4,9	4,8	4,6	4,6	4,7	4,8	4,7	4,9
COMPRESSORS	VERDICHTER		nr.	1	1	1	1	1	1	1	1	1	1	1
REFRIGERATING CIRCUITS	KÄLTEKREISLÄUFE		nr.	1	1	1	1	1	1	1	1	1	1	1
PARTITION STEP	LEISTUNGSSTUFEN		nr.	1	1	1	1	1	1	1	1	1	1	1
REFRIGERANT	KÄLTEMITTEL		R	R410A										
HYDRAULIC SECTION	**HYDRAULIKMODUL**													
NOMINAL WATER FLOW	VOLUMENSTROM		m3/h	0,3	0,4	0,6	0,7	0,9	1,4	1,6	2,1	2,3	3,1	3,8
WATER FLOW RANGE	WASSERDURCHSATZ		m3/h	0,3 ÷ 2	0,3 ÷ 2	0,6 ÷ 2,2	0,6 ÷ 2,2	0,8 ÷ 2,2	1,2 ÷ 2,4	1,4 ÷ 3	1,2 ÷ 2,9	1,2 ÷ 2,9	2,5 ÷ 5	3 ÷ 6
TYPE OF EVAPORATOR	VERDAMPFERTYP			Plate evaporator *Plattenverdampfer*		Self - cleaning coaxial evaporator *Selbstreinigungs Koaxial Verdampfer*								
EVAPORATOR PRESSURE DROP	VERDAMPFER DRUCKVERLUST		kPa	20	22	22	23	23	26	25	27	28	28	31
AVAILABLE PRESSURE	BETRIEBSDRUCK	P3	kPa	301	294	279	269	252	262	270	263	264	249	241
MAXIMUM PUMP ABSORBED POWER	LEISTUNGSAUFNAHME PUMPE	P3	kW	0,56	0,56	0,56	0,56	0,56	0,98	0,98	0,98	0,98	0,98	1,28
MAXIMUM PUMP ABSORBED CURRENT	STROMAUFNAHME PUMPE	P3	A	3,46	3,46	3,46	3,46	3,46	1,78	1,78	1,78	1,78	1,78	2,37
AVAILABLE PRESSURE	BETRIEBSDRUCK	P5	kPa	-	-	431	421	401	611	593	562	492	570	518
MAXIMUM PUMP ABSORBED POWER	LEISTUNGSAUFNAHME PUMPE	P5	kW	-	-	0,74	0,74	0,74	1,10	1,10	1,10	1,10	1,47	1,47
MAXIMUM PUMP ABSORBED CURRENT	STROMAUFNAHME PUMPE	P5	A	-	-	3,22	3,22	3,22	2,17	2,17	2,17	2,17	2,86	2,86
HYDRULIC CONNECTIONS	WASSERANSCHLÜSSE		BSP/DN	1/2"	1/2"	3/4"	3/4"	3/4"	1"	1"	1"	1"	1"	1"
TANK VOLUME	WASSERINHALT		dm3	10	10	40	40	40	50	50	50	50	110	110
EXPANSION VESSEL VOLUME (3)	EXPANSION BEHÄLTERVOLUMEN (3)		liters	N.A.					5				8	
FAN SECTION (AXIAL)	**AXIALVENTILATOREN**													
TOTAL AIR FLOW	NENNLUFTMENGE		m3/h	700	650	1300	1200	1500	4100	4100	4750	4750	6500	7400
FANS	ANZAHL LÜFTER		nr.	1	1	1	1	1	1	1	1	1	1	1
FANS ABSORBED POWER	LEISTUNG LÜFTER		kW	0,07	0,11	0,09	0,09	0,10	0,25	0,25	0,49	0,49	0,68	0,81
FANS ABSORBED CURRENT	LÜFTER STROMAUFNAHME		A	0,4	0,8	0,4	0,4	0,5	1,1	1,1	2,4	2,4	3,0	1,5
TOTAL ELECTRIC DATA	**GESAMT STROMDATEN**			IP54 protection rating, chillers suitable for outdoor installation Schutzart IP54										
NOMINAL ABSORBED POWER (4)	LEISTUNGSAUFNAHME (OHNE PUMPE) (4)		kW	1,1	1,4	1,9	2,1	2,5	3,8	4,6	5,4	6,7	7,5	8,8
MAXIMUM ABSORBED CURRENT(F.L.A.) (4)	MAX. BETRIEBSSTROM (F.L.A.) (4)		A	6,1	7,5	9,6	10,5	12,5	10,1	10,5	13	13,9	18,8	19,8
MAXIMUM PEAK CURRENT (L.R.A.) (4)	MAX. ANLAUFSTROM (L.R.A.) (4)		A	16	21	27	40	46	50	50	71	71	75	104
ELECTRIC FEED	**ELEKTRISCHE EINSPEISUNG**		V/Ph/Hz	230/1/50					400/3/50/N					400/3/50
NOISE DATA	**GERÄUSCHE**													
SOUND PRESSURE (2) (4)	SCHALLDRUCKLEISTUNG(2) (4)		dB(A)	51	51	51	51	51	51	51	52	52	53	55,8
DIMENSIONS AND WEIGHT	**ABMESSUNGEN UND GEWICHT**													
LENGTH	LÄNGE		mm	445	445	600	600	600	820	820	820	820	1010	1010
WIDTH	BREITE		mm	440	440	655	655	655	615	615	615	615	720	720
HEIGHT	HÖHE		mm	740	740	1035	1035	1035	1360	1360	1360	1360	1580	1580
WEIGHT EMPTY	LEERGEWICHT		kg	55	55	85	90	95	160	165	170	175	210	260
WEIGHT OPERATING	BETRIEBSGEWICHT (OHNE PUMPE UND OHNE WASSERINHALT)		kg	65	65	125	130	135	210	215	220	225	340	390

The manufacturer reserves the right to modify specifications without notice. *Der Hersteller behält sich das Recht vor, Spezifikationen ohne vorherige Ankündigung zu ändern.* updated on 22/05/2018

Figure 41- Hitema Technical Data of ENR chillers.

ENFRIADORAS DE AGUA SERIE ENR

Con depósito y bomba. Intercambiador coaxial (hasta 120Kw) o multitubular (resto de serie).
R410A. Compresores Scroll.

MODELO	Potencia frigorífica	Potencia nominal absorbida	C.O.P.	Nivel sonoro	Conexiones de agua	Dimensiones	Peso
	kW	kW	Kw/kW	dB(A)	BSP / DN	LargoxAnchoxAlto	Kg
ENR 022	22	13.7	3.2	53.4	1 ½ "	1610x860x1480	390
ENR 030	31	18.5	3.6	52.6	1 ½ "	1610x860x1480	400
ENR 038	38	20.7	3.3	54.5	1 ½ "	1610x860x1480	430
ENR 045	43	23.4	3.2	54.8	1 ½ "	1610x860x1480	450
ENR 061	60	35.2	3.5	55.1	2"	2220x1011x1990	710
ENR 075	75	39.5	3.3	57.1	2"	2220x1011x1990	800
ENR 085	85	46.6	3.3	57.9	2"	2220x1011x1990	815
ENR 120	119	70.7	3.2	56.4	2"	3310x1100x2110	1265
ENR 150	150	79.3	3	59.3	DN65	3310x1100x2110	1440
ENR 170	162	91.6	2.9	59.7	DN65	3310x1100x2110	1595
ENR 230	229	120.3	3.2	62.2	DN65	5010x1100x2105	1915
ENR 280	281	163.1	2.9	62.6	DN125	5010x1100x2105	2115
ENR 330	326	169.5	2.8	64.9	DN125	5010x1100x2105	2160

Temperatura de entrada agua 12º C, temperatura de salida del agua 7º C, temperatura ambiente 35º C
Niveles de presión Sonora medidas según normativa ISO03744

Figure 42- Equifab Technical Data of ENR chillers.

Appendix E: Technical Drawing of a Pump

In this appendix, a technical drawing of an oil pump is illustrated in figure 38.

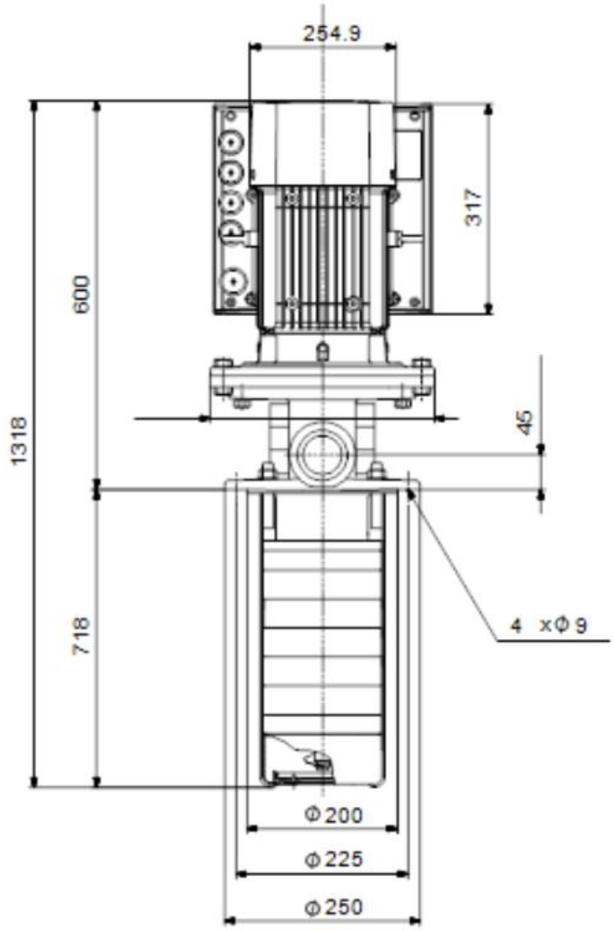

Figure 43- Technical drawing of a pump.

Appendix F: Characteristic Curves of the Pumps

In this last annex are present all the characteristic curves of the pumps mentioned throughout the dissertation.

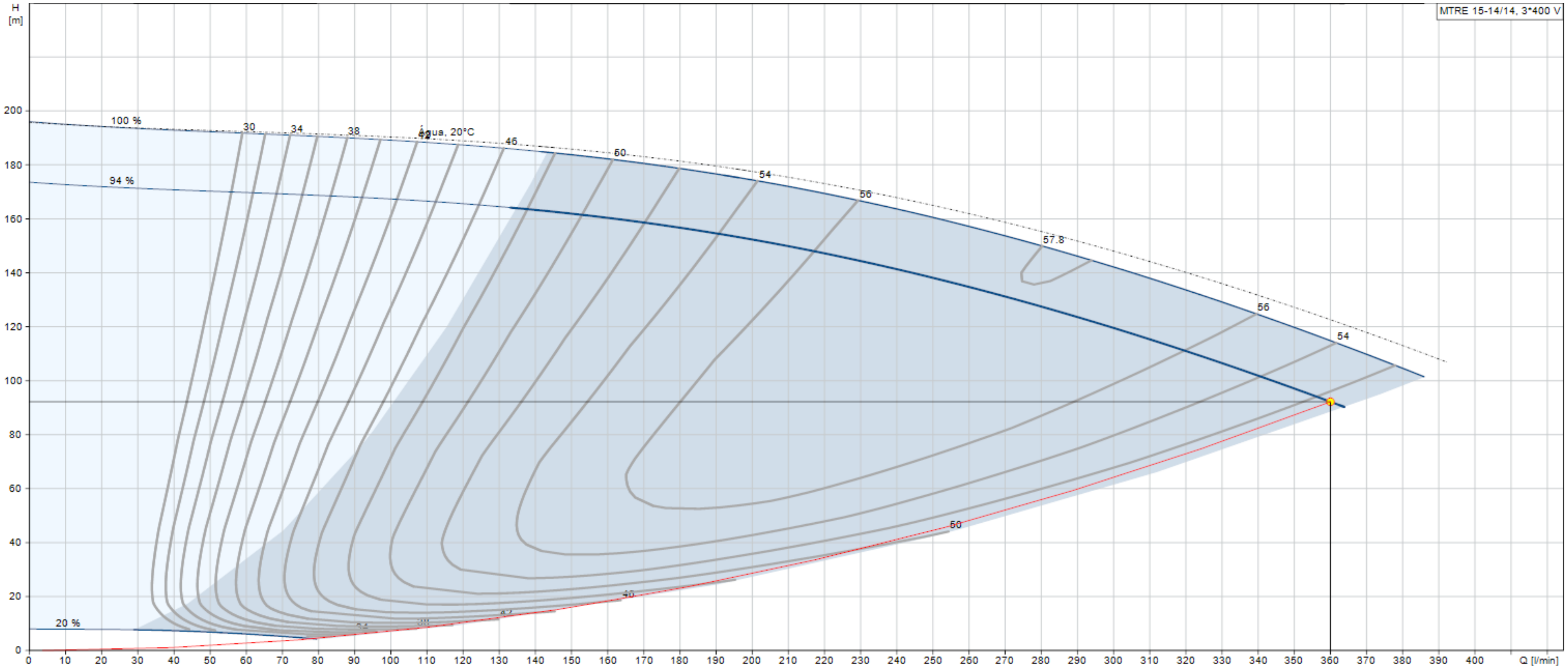

Figure 44 - Characteristic curve of Grundfos MTRE 15-14/14 pump.

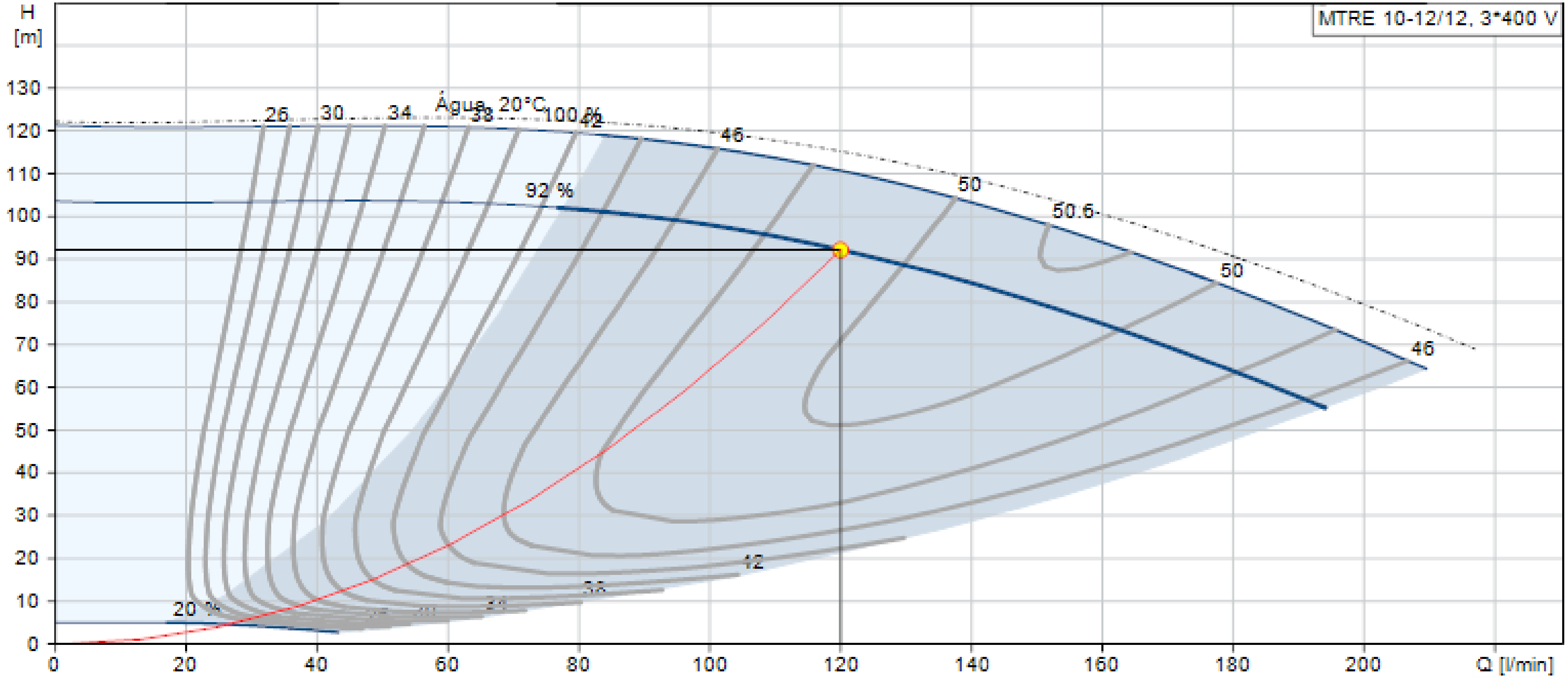

Figure 45 - Characteristic curve of Grundfos MTRE 10-12/12 pump.

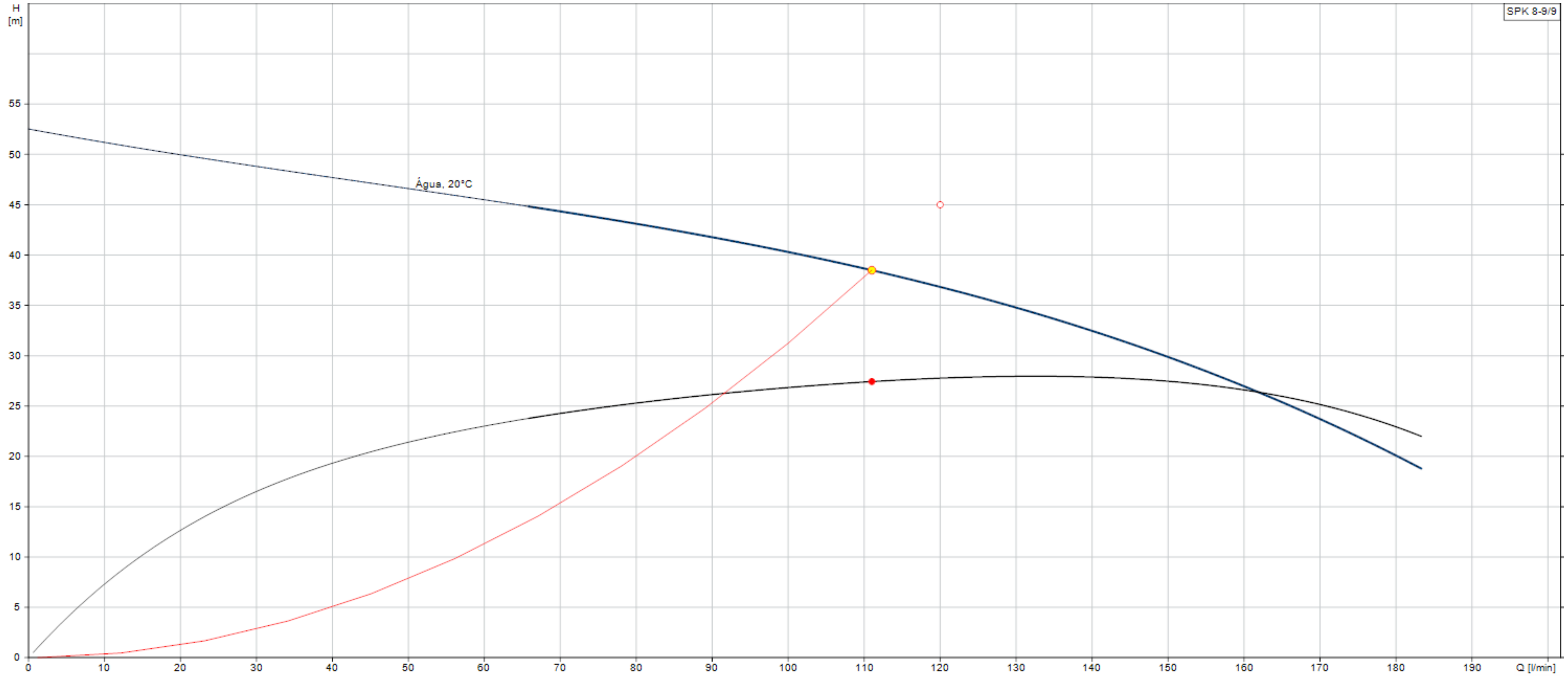

Figure 46 - Characteristic curve of Grundfos SPK8-9/9 pump.

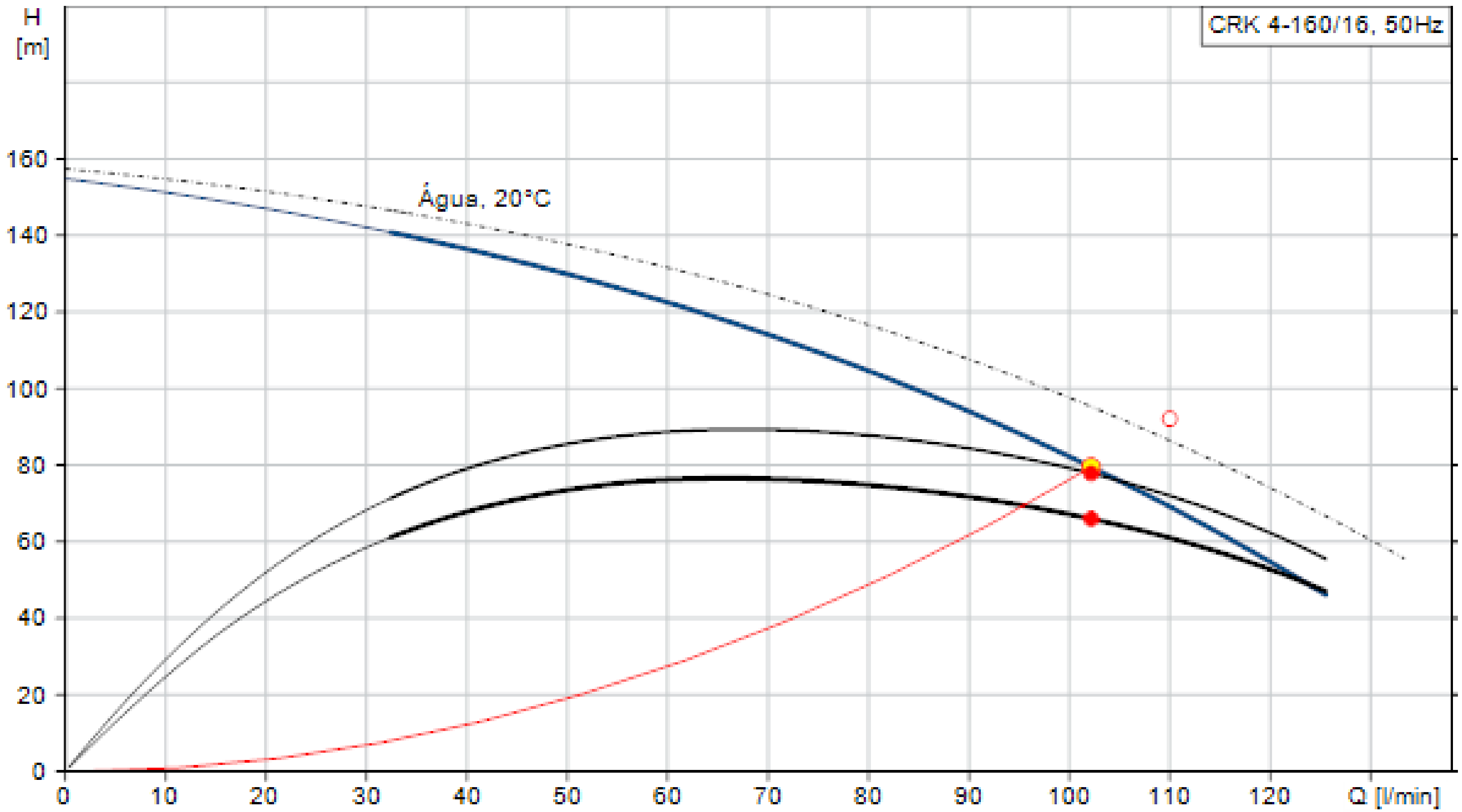

Figure 47 - Characteristic curve of Grundfos CRK4-160/16 pump.

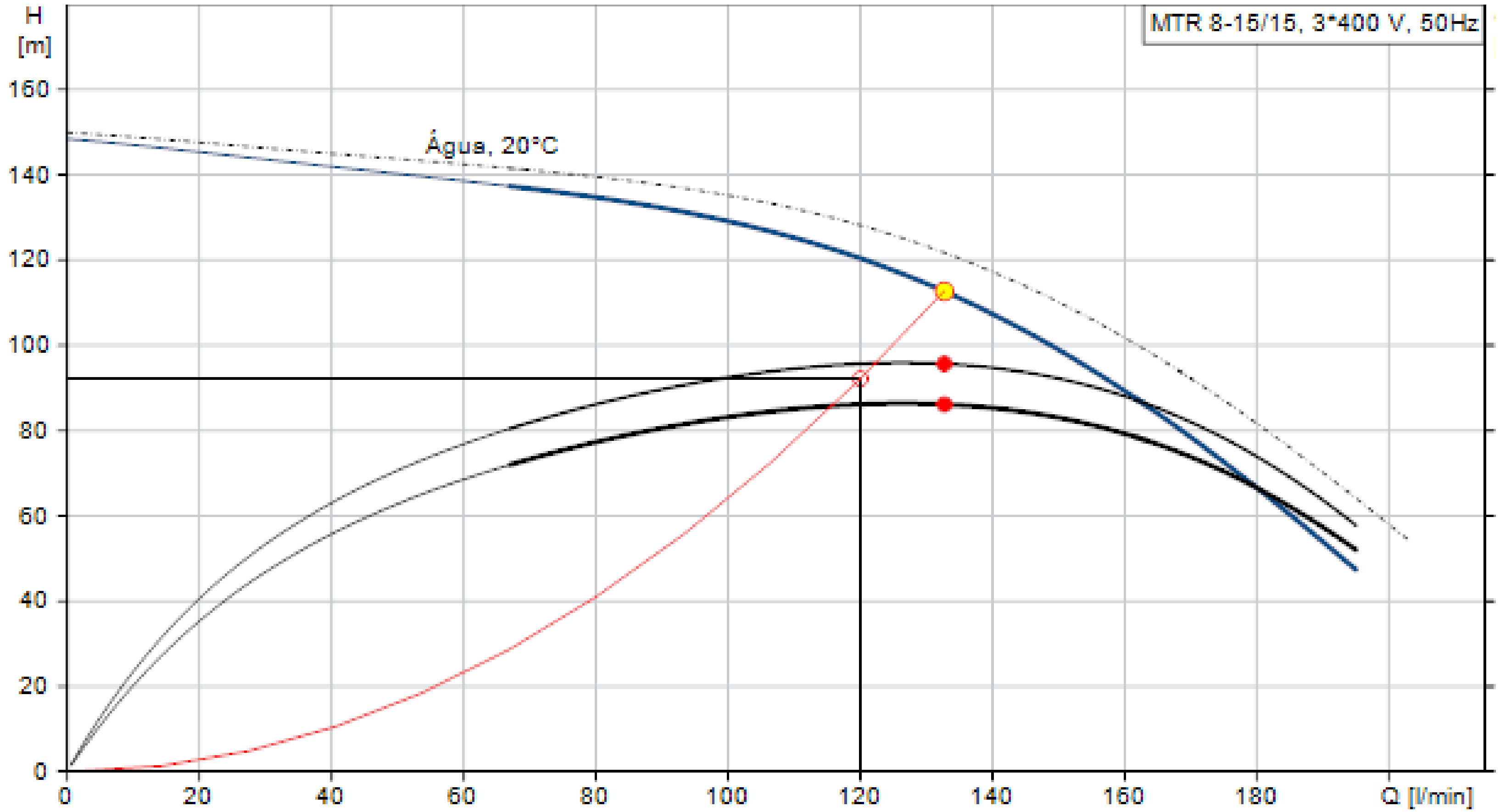

Figure 48 - Characteristic curve of Grundfos MTRE 8-18/15 pump.

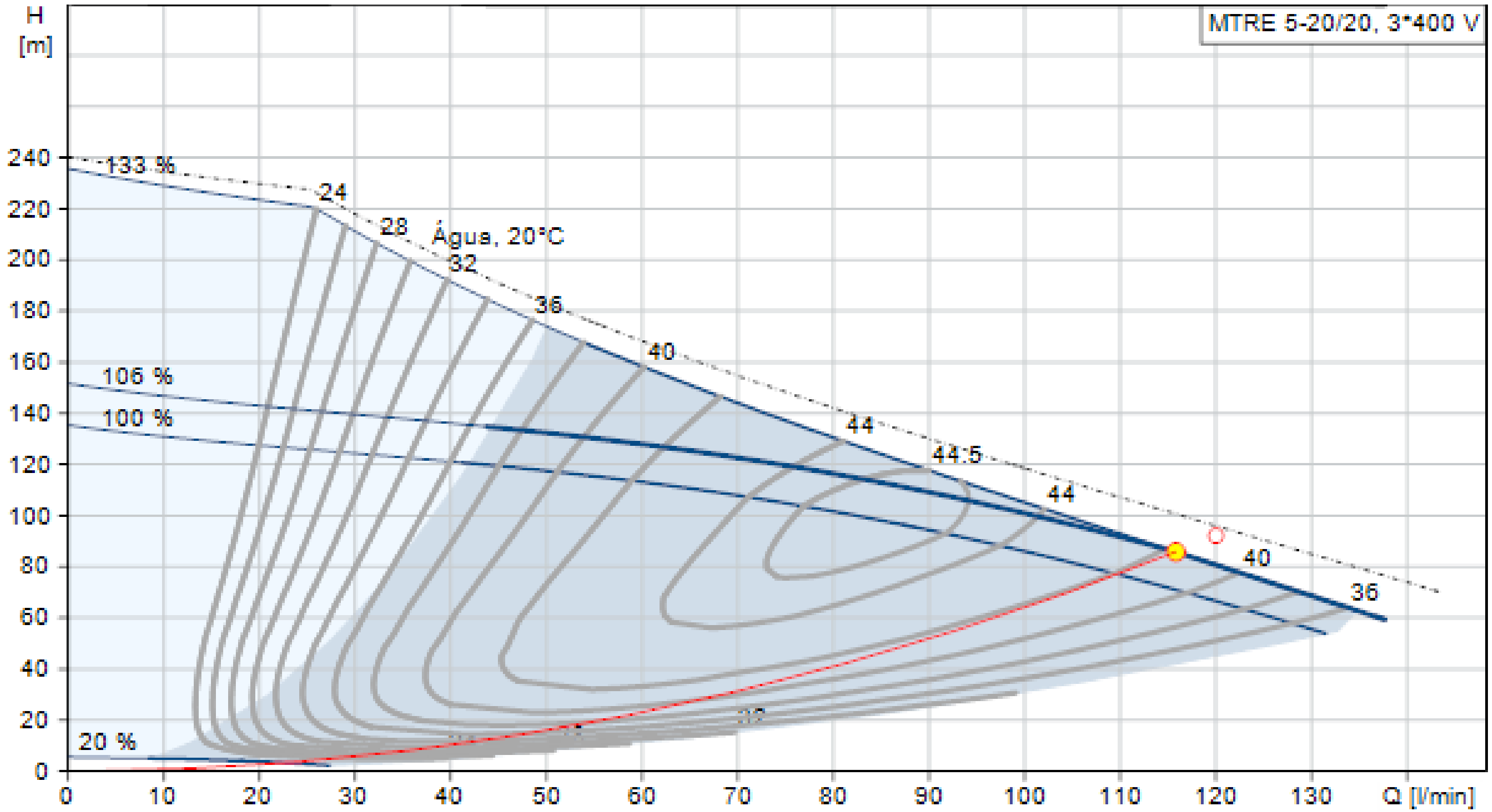

Figure 49 - Characteristic curve of Grundfos MTRE 5-20/20 pump.

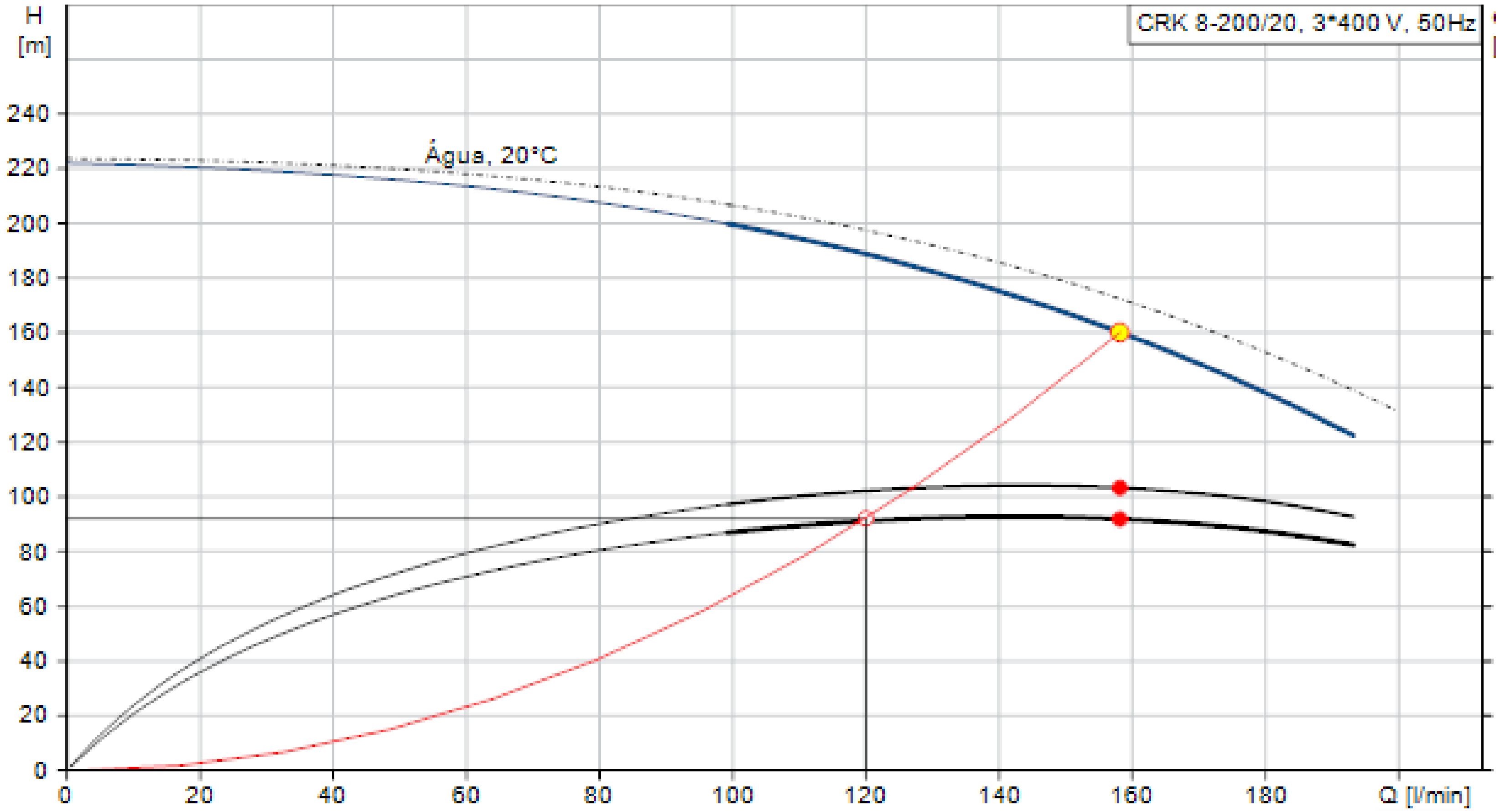

Figure 50 - Characteristic curve of Grundfos CRK8-200/20 pump.

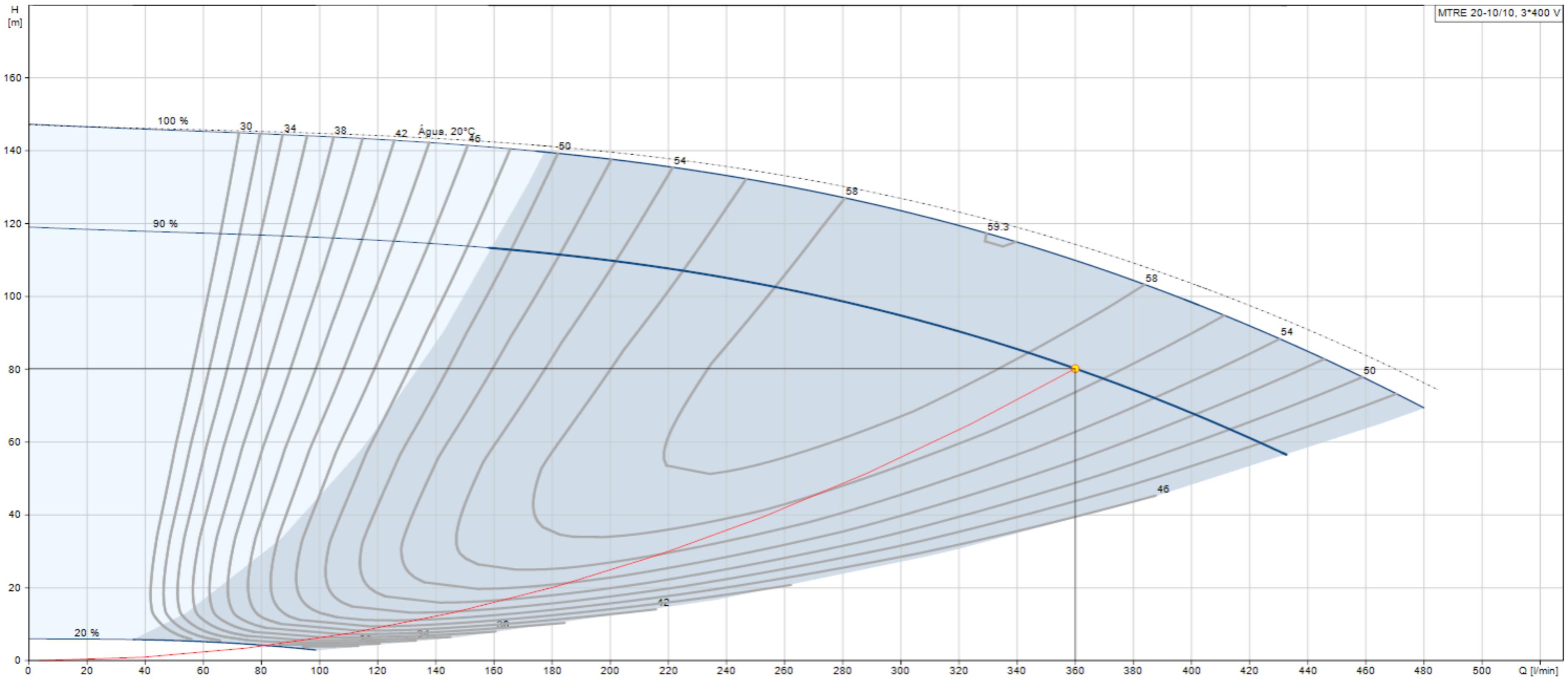

Figure 51 - Characteristic curve of Grundfos MTRE 20-10/10 pump.

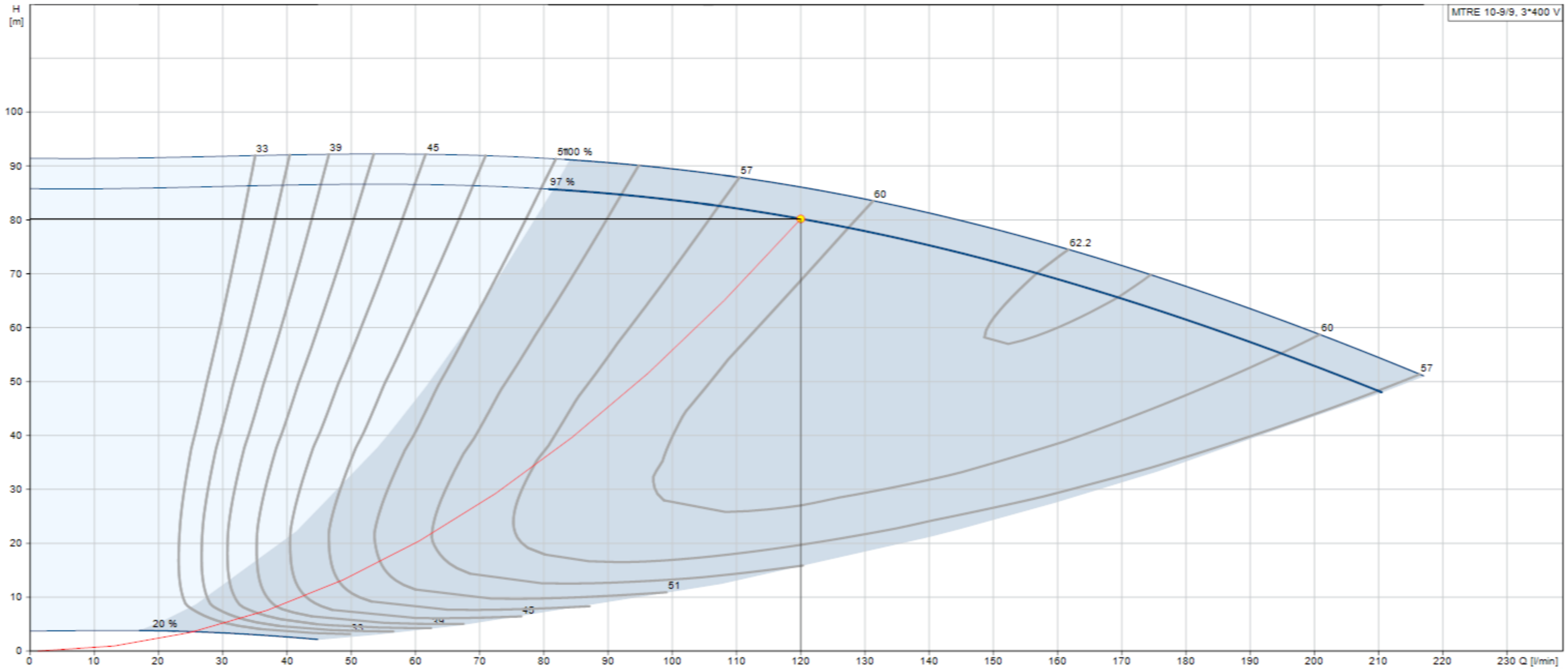

Figure 52 - Characteristic curve of Grundfos MTRE 10-9/9 pump.

Table 22 - Features of oil return pumps available from the Xylem company [25].

Model	Power [kW]	Weight [Kg]	[m³/h] 0	7,2	12	14,4	18	21
			[l/min] 0	120	200	240	300	350
			H = M.C.O.					
CO 350/03/A	0,37	8	9,5	6,3	4,8	4,1	3	
CO 350/05/A	0,55	11	12	8,8	7,1	6,3	5,1	4
CO 350/07/D	0,75	14	13,7	10,8	9,1	8,2	6,9	5,8
CO 350/09/D	0,9	16	15,7	12,2	10,5	9,6	8,3	7,2
CO 350/11/D	1,1	15	17,3	13,8	12	11,2	10,1	9,1
CO 350/15/D	1,5	18	20,3	16,4	14,4	13,5	12,2	11,2

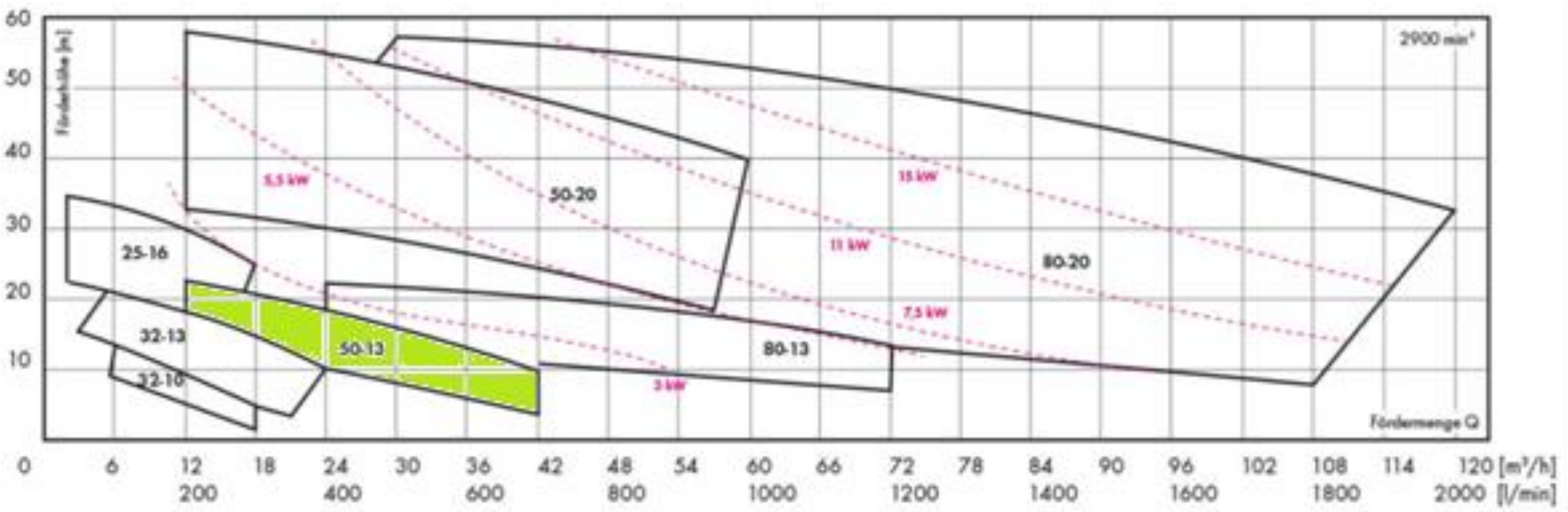

Figure 53- Performance characteristics of existing pumps in the German company (Schmalenberger 2022).